June 2019

Living Shorelines As Alternative Methods Of Shoreline Protection

Hunter Shows
hshows1@lsu.edu

LIVING SHORELINES AS ALTERNATIVE METHODS OF SHORELINE PROTECTION

A Thesis

Submitted to the Graduate Faculty of the
Louisiana State University and
Agricultural and Mechanical College
in partial fulfillment of the
requirements for the degree of
Master of Science

in

The Department of Civil and Environmental Engineering

by
Hunter Joseph Shows
B.S., Louisiana State University, 2016
August 2019

ACKNOWLEDGMENTS

I would like to thank my advisor, Dr. Clint Willson, for his help and guidance in my graduate school career. I would also like to thank Dr. Bret Webb whose guidance helped me greatly over the past two years. I would like to thank my committee members, Dr. Navid Jafari and Dr. Robert Twilley for their time and commitment to helping me along the way. I would also like to thank Tommy McGinnis and the folks with the Coastal Protection and Restoration Authority for their help understanding and assessing the CPRA documents utilized in this project.

I am very thankful for my parents, Neil and Pam Shows, who have helped and supported me throughout my entire academic career and always pushed me to achieve my best. I would like to thank all my other friends and family who have assisted me throughout my studies.

TABLE OF CONTENTS

ACKNOWLEDGMENTS ii

LIST OF TABLES v

LIST OF FIGURES vi

ABSTRACT viii

1. INTRODUCTION 1
   1.1. BACKGROUND AND REGIONAL INFORMATION 1

2. LITERATURE REVIEW 6
   2.1. OYSTER REEF CHARACTERISTICS 6
   2.2. TRADITIONAL BREAKWATER VS. ENGINEERED LIVING SHORELINE 8
   2.3. WAVE TRANSMISSION 9
   2.4. EFFECTS ON SEDIMENT TRANSPORT 11

3. OBJECTIVES / METHODS 14

4. CALCULATIONS 15
   4.1. POROSITY COEFFICIENT 15
   4.2. SOIL VOLUME CHANGE RATE 15
   4.3. WAVE TRANSMISSION 16

5. PROJECT MONITORING SUMMARIES 18
   5.1. LA-0016 18
   5.2. PO-0148 21
   5.3. LA-0008 25
   5.4. TE-0045 28

6. RESULTS 36
   6.1. POROSITY COEFFICIENT 36
   6.2. TRANSMISSION COEFFICIENT 42

7. DISCUSSION 48

8. CONCLUSION 53

REFERENCES 55

APPENDIX A. VOLUMETRIC CHANGE RATE EXAMPLE FIGURES 60

APPENDIX B. EXAMPLE CALCULATIONS 66

VITA 68

LIST OF TABLES

Table 1. Empirical wave runup prediction coefficients for smooth impermeable slopes (Seelig 1980). 10

Table 2. LA-0016 project monitoring summary and calculated Porosity Coefficient (*Cp*) 21

Table 3. PO-0148 project monitoring summary and calculated Porosity Coefficient (*Cp*) 24

Table 4. LA-0008 project monitoring summary and calculated Porosity Coefficient (*Cp*) 28

Table 5. TE-0045 project monitoring summary and calculated Porosity Coefficient (*Cp*) for Reach A, Reach B, and Reach E 32

LIST OF FIGURES

Figure 1. CPRA Coastal Master Plan, 2017 1

Figure 2. CPRA Coastal Master Plan Interactive Project Map, 2017 2

Figure 3. Locations of Study Sites Along the Louisiana Gulf Coast 4

Figure 4. LA-0016 shoreline protection structures and reference locations (McGinnis, 2018) 18

Figure 5. WSS installed in Vermilion Bay for LA-0016 (left) and WSS drawing (right) (McGinnis, 2018) 19

Figure 6. WAD®s As-Built Drawing (top) and WAD®s installed in Vermilion Bay (bottom) for LA-0016 (McGinnis 2018) 19

Figure 7. ESUs stacked before instilation and pile insertion (left) and ESUs installed in Vermilion Bay (right) for LA-0016 (McGinnis 2018) 20

Figure 8. Drawing of BCECMS (left) and installed BCECMS (right) in Vermilion Bay for LA-0016 (McGinnis 2018) 20

Figure 9. PO-0148 shoreline protection structures and reference locations (Chauvin, 2018) 22

Figure 10. Reef Ball Type 1 (left) and 2 (right) conceptual drawings, (Coast and Harbor Engineering, 2015) 22

Figure 11. Reef Ball Type 2 (right) and 1 (left) deployed at PO-0148 project site (Chauvin, 2018) 23

Figure 12. WAD®s installed at PO-0148 (left) and conceptual drawing of WAD®s used at PO-148 (Chauvin, 2018; Coast and Harbor Engineering, 2015) 23

Figure 13. OysterBreak™ installed at PO-0148 (left) and concpetual drawing of OysterBreak™ for PO-0148 (Chauvin, 2018; Coast and Harbor Engineering, 2015) 24

Figure 14. LA-0008 project location and reference area (McGinnis, 2017) 26

Figure 15. Oysterkrete© breakwater (top) and Standard Weight Oysterbreak™ aerial imagery from 2014 (McGinnis 2017) 27

Figure 16. TE-0045 project location and reference area (Melancon et al. 2015) 29

Figure 17. A-Jack Treatment at TE-0045 project site (top) and project completion report drawing of A-Jack Treatments (bottom) (Melancon et al. 2015; TBS Project Completion Report, 2008) 30

Figure 18. ReefBLKTreatment at TE-0045 project site (top) and project completion report drawing of ReefBLK Treatments (bottom) (Melancon et al. 2015; TBS Project Completion Report, 2008) 31

Figure 19. Reach A of TE-0045 structure location and reference area (Melancon et al. 2015) 33

Figure 20. Reach B of TE-0045 structure location and reference area (Melancon et al. 2015) 34

Figure 21. Reach E of TE-0045 structure location and reference area (Melancon et al. 2015) 35

Figure 22. Porosity Coefficient versus Soil Volume Change Rate ($yd^3\ ac^{-1}\ yr^{-1}$) for project PO-0148 37

Figure 23. Porosity Coefficient versus Soil Volume Change Rate ($yd^3\ ac^{-1}\ yr^{-1}$) for project LA-0016 37

Figure 24. Porosity Coefficient versus Soil Volume Change Rate ($yd^3\ ac^{-1}\ yr^{-1}$) for project TE-0045 Reach A (Blue Triangle), Reach B (Orange Square), and Reach E (Grey Circle) 39

Figure 25. Porosity Coefficient versus Soil Volume Change Rate ($yd^3\ ac^{-1}\ yr^{-1}$) for project LA-0008 40

Figure 26. Study wide Porosity Coefficient versus Soil Volume Change Rate ($yd^3\ ac^{-1}\ yr^{-1}$) for all structures 41

Figure 27. Transmission Coefficient versus Soil Volume Change Rate ($yd^3\ ac^{-1}\ yr^{-1}$) for project PO-0148, Water level -0.5 (Grey Square) and Water Level 1.0 (Blue Circle) 43

Figure 28. Transmission Coefficient versus Soil Volume Change Rate ($yd^3\ ac^{-1}\ yr^{-1}$) for project LA-0016 43

Figure 29. Transmission Coefficient versus Soil Volume Change Rate ($yd^3\ ac^{-1}\ yr^{-1}$) for project LA-0008 for 2012 monitoring (Orange Square) and 2014 monitoring (Blue Circle) 44

Figure 30. Study wide Transmission Coefficient versus Soil Volume Change Rate ($yd^3\ ac^{-1}\ yr^{-1}$) for all structures 46

Figure 31. Study wide Transmission Coefficient versus Soil Volume Change Rate ($yd^3\ ac^{-1}\ yr^{-1}$) for all structures (Logarithmic) 47

Figure 31. CRMS Monitoring Stations in relation to shoreline protection study sites 52

ABSTRACT

Louisiana's marshes and coastal estuaries are losing habitat at an alarming rate. High rates of sea level rise coupled with coastal subsidence are turning once thriving marsh land into open water. The sediment starved Mississippi River Delta is drowning, making families homes, property, and livelihoods increasingly vulnerable every year. Significant funding is being allocated for projects to offset the increasing erosion including but not limited to diversions, marsh creation, ridge restoration, and shoreline protection projects.

Living shorelines, for the sake of this study, can be defined as a form of shoreline protection which helps shoreline stabilization and erosion reduction while still providing estuarine habitat and other ecosystem services. Living shorelines offer an eco-friendly alternative to traditional shoreline protection measures which can be costly, offer little ecosystem services, and often become ineffective by sinking below water level due to highly compactable bottom sediments. This study investigates some of the living shoreline projects completed along the Louisiana coast for porosity and wave attenuation and the subsequent effect on volumetric soil erosion rates. Wave attenuation, while important for reducing wave energy in the shoreward regions, did not show a strong correlation with volumetric erosion rates. However, increasing porosity, ranging from 0% to 35%, was shown to have a relationship with soil volume change rates in that the more porous a structure was, less erosion, and in some cases accretion, was shown across all projects.

1. INTRODUCTION

1.1. BACKGROUND AND REGIONAL INFORMATION

The Louisiana coast is a prized possession that bring millions of dollars in revenue every year through commercial fishing, tourism, and oil and gas exploration and production. The wetlands found on Louisiana's coast are home to some of the most productive coastal estuaries found in the United States. These estuaries, however, are in danger of vanishing due to sea level rise, subsidence, and erosion. Louisiana's wetlands make up about forty percent of the nation's wetlands yet account for approximately eighty percent of the wetland losses (USGS Fact Sheet, 1995). According to the Louisiana Coastal Protection and Restoration Authority (CPRA) 2017 Coastal Master Plan, numerical models of land change show that the previous worst-case scenario for land loss in the state of Louisiana has become the new best case for the next 50 years with no coastal protection or restoration projects (Figure 1).

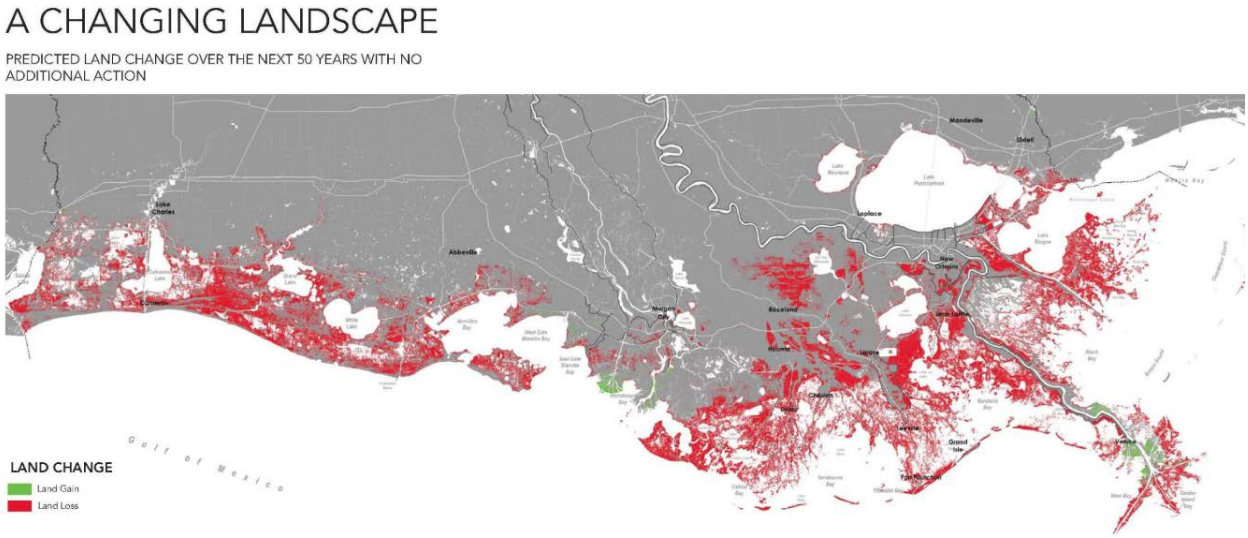

Figure 1. CPRA Coastal Master Plan, 2017

In addition to natural processes, human activities have greatly accelerated the rate of land loss in coastal Louisiana. The leveeing of the Mississippi River and its distributaries for flood control and navigation has deprived the sediment dependent coast of its main source of deposition

(USGS Fact Sheet, 1995). Furthermore, dredging of wetlands for oil and gas pipeline canals has restricted or cut off surface hydrology, preventing tidal ebb and flow and effectively drowning wetlands (Turner 1985). Efforts have been and are currently being made to mitigate for natural and manmade impacts to Louisiana's wetlands, with billions of dollars being spent on restoration and preventative action projects (CPRA Coastal Master Plan, 2017). As shown in Figure 2, diversions, marsh creation, barrier island / headland restoration, hurricane protection, hydrologic restoration, and shoreline protection projects are being engineered, designed, and constructed at a much higher priority and pace than in Louisiana's history (CPRA Coastal Master Plan, 2017).

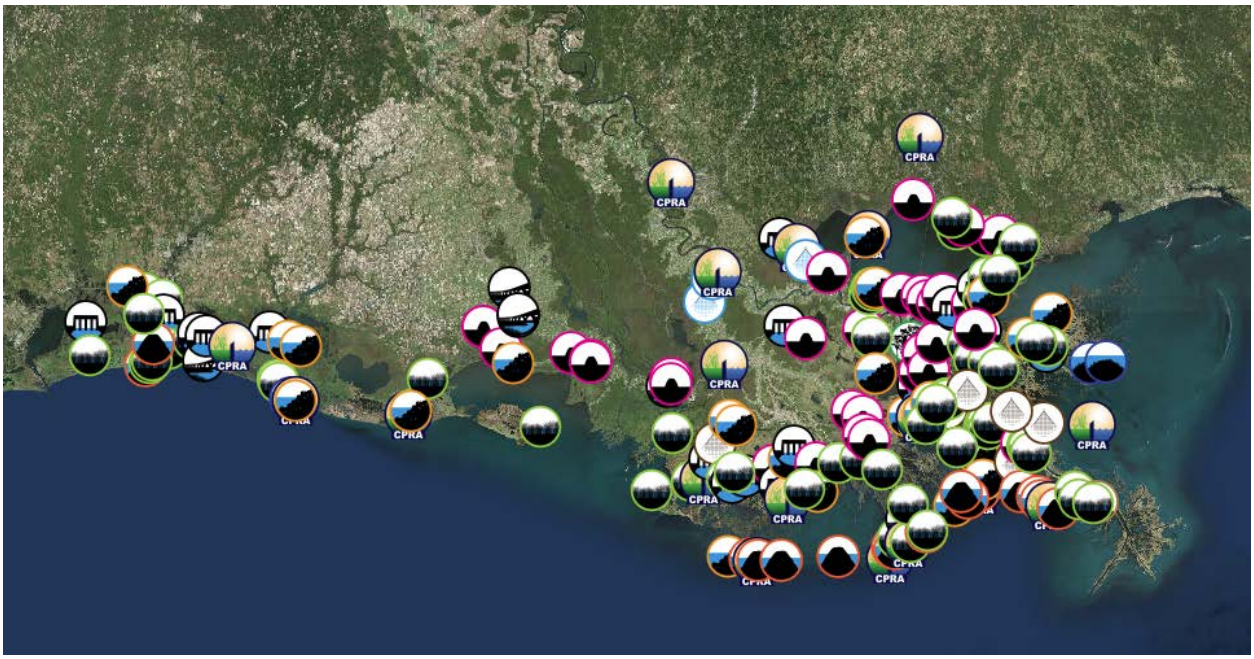

Figure 2. CPRA Coastal Master Plan Interactive Project Map, 2017

Implementation of oyster reefs for the use of shoreline protection has become a large focus (among others) in the state of Louisiana to offset the accelerating deterioration of coastal marsh habitat and shoreline erosion, as well as supplement oyster habitat and settlement. These efforts include four completed oyster barrier reef restoration / living shoreline projects featured in the

Master Plans created by CPRA, and several completed by other non-profit organizations such as the Coalition to Restore Coastal Louisiana (CRCL) among others with individual fund raising efforts, donations, and others with funds from the federal government such as the Coastal Wetlands Planning, Protection and Restoration Act (CWPPRA) (CPRA 2017, CRCL). Oyster reefs act as a form of green infrastructure that not only serves as shoreline protection such as typical breakwaters or other styles of "hard infrastructure", but also benefit the ecosystem by providing habitat for smaller aquatic species. They also reduce turbidity through suspension bivalve feeding, promoting growth of submerged aquatic vegetation (SAV) which can also contribute to wave attenuation and sediment retention (Davis et al. 2015; Reidenbach et al. 2013; Smith et al. 2009). Several research studies have been conducted in laboratory environments, with numerical computer models, and with physical field observations and data collection with the goal of quantitatively defining the importance of oyster reefs on the surrounding ecosystem.

The study sites analyzed in this project consist of four shoreline protection projects completed by CPRA in Coastal Louisiana (Figure 3). They are titled PO-0148, LA-0016, TE-0045, and LA-0008. The name of each of the four projects are as follows:

1. PO-0148- Living Shoreline Demonstration Project (November 2016)
2. LA-0016- Non-Rock Alternatives to Shoreline Protection (November 2015)
3. TE-0045- Terrebonne Bay Shore Protection Demonstration (December 2007)
4. LA-0008- Bio-Engineered Oyster Reef Demonstration Project (February 2012)

The PO-0148 project is located in Biloxi Marsh and was completed in November 2016. The project created 3.1 miles of artificial reef comprised of WAD® (Wave Attenuation Device), Reef Balls, ReefBLK, and Oysterbreak™ structures (PO-148 Fact Sheet). LA-00016 is located in Vermilion Bay and was completed in November of 2015. The project created 4,500 linear feet of

artificial reef comprised of WAD®s (Wave Attenuation Devices), WSS (Wave Screen Systems), ESUs (Ecosystem Units), and Buoyancy Compensated Erosion Control Modules (BCECMS) (McGinnis, II, T.E. 2018). TE-0045 is located in Terrebonne Parish and was constructed in December of 2007. The project created three separate shoreline protection reaches containing A-Jack, Gabion Mat, and ReefBLK structures (Melancon, E. J. Jr. et al., 2015). The last project analyzed is LA-0008, located on the northern shoreline of the Gulf of Mexico in the Rockefeller Wildlife Refuge. This project was constructed in February of 2012 and is comprised of two 215 feet long concrete Oysterbreak™ sections, one with low density OysterKrete© concrete (McGinnis, II, T. E., 2017). Overall, these projects contain eleven different alternative living shoreline methods to shoreline protection.

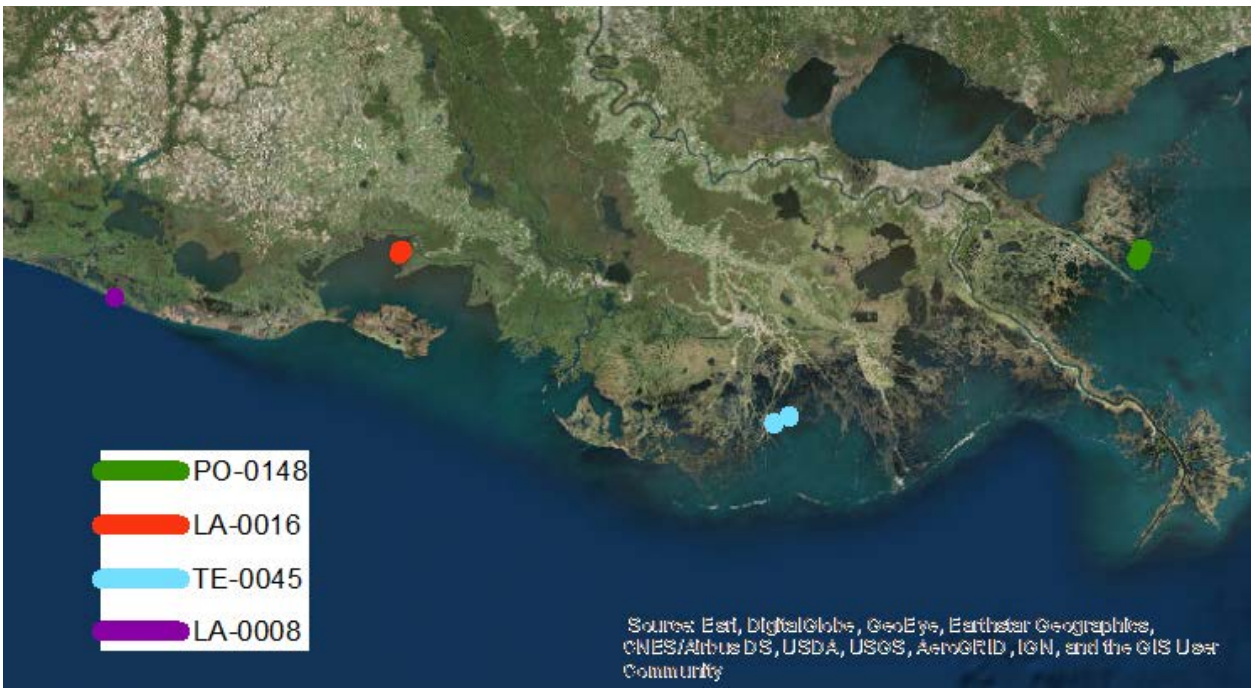

Figure 3. Locations of Study Sites Along the Louisiana Gulf Coast

Each of these projects were completed with different goals in mind. For example, the TE-0045 project was implemented to abate shoreline erosion and develop and sustain an oyster reef,

not to attenuate wave energy (Melancon, E. J. Jr. et al., 2015). The LA-0008 project was designed to address shoreline erosion issues in an environment with highly compactible bottom sediments, provide oyster habitat, and compare the OysterKrete© structure to the standard weight concrete structures (McGinnis, II, T. E., 2017). The LA-0016 demonstration project was proprietary in nature, with the primary goal being to assess alternative methods of shoreline protection by private firms (McGinnis, II, T.E. 2018). The main goal of the PO-0148 project's primary goal was to combat shoreline erosion (Chauvin 2018). In this study, these four projects are analyzed not on the project specific goals, but on the trends found between porosity, wave attenuation, and erosion.

2. LITERATURE REVIEW

2.1. OYSTER REEF CHARACTERISTICS

Oyster reefs along the Gulf coast are comprised of the eastern oyster (*Crassostrea virginica*), existing as either subtidal or intertidal three-dimensional structures where oysters colonize and reproduce, continuously growing the reef both horizontally and vertically (Puglisi, 2008). Juvenile oysters, or spat, use the hard shells of living or deceased oysters for habitat as they settle and search for cover. The recruitment of spat to existing oyster reefs, and the growth of spat into oysters having hard shells drives the vertical and horizontal expansion of the reef itself, becoming larger with each generation of oysters (Burrows et al., 2005).

Oysters function as suspension feeders, filtering the water column at rates up to 100 L individual oyster^{-1} day^{-1} in order to consume sufficient amounts of organic phytoplankton as food (Riisgard 1988). Filtering at this capacity can help to trap and recycle nutrients essential to coastal ecosystems, making oysters a vital part of a healthy environment conducive to ecosystem production (Burrows et al. 2005). The filter feeding mechanism of oysters also helps to increase the settlement rate of suspended sediments as oysters discard inorganic particles to the seafloor that are either too big or small for consumption as pseudo feces**,** decreasing the turbidity of the water column (Burrows et al. 2005; Meyer and Townsend 2000, Nelson et al. 2004). Oysters can also provide an increase in sediment deposition by lowering bed shear stress below the critical value for resuspension, and also by deposition due to bivalve feeding (Reidenbach et al. 2013). Reducing the turbidity of the water column helps to prevent light attenuation at the benthic layer, which promotes the growth of submerged aquatic vegetation, which also helps to reduce turbidity by trapping (Reidenbach et al. 2013). The positive feedback loop coupling turbidity reduction by living oyster reefs promoting the growth of submerged aquatic vegetation (SAV)

further helps to stabilize mud flat bottoms and marsh edge where the SAV is rooted. This shows the importance of the role of oyster reefs and their restoration as a water column filter when considering marsh restoration projects of all varieties, such as marsh creation from dredged sediment, where turbidity in the water column may be very high, and seeded or natural SAV may be struggling to emerge (McGlathery et al. 2012).

Oyster reefs also provide excellent structure and habitat for organisms other than the oysters themselves, being that they are often the only hard structure available in areas dominated by mud flats and SAV patches (Schulte et al., 2009). Numerous animals are dependent on oyster reefs for habitat such as crabs and other natural predators of oysters. The reefs also provide structure for fish who use the area as feeding grounds preying on invertebrates and crustaceans or breeding grounds for spawning. Vegetation is also very common in and around oyster reefs providing food for various coastal species, and also contributing to sediment deposition and primary production of the ecosystem as a whole (Burrows et al. 2005).

Oyster reefs also serve as an important factor in reducing shoreline erosion. The reefs function in a similar fashion to rock breakwaters, dampening wave energy by inducing wave breaking as the wave trains propagate over the reef. This filtering prevents higher frequency waves from entering coastal marshes by attenuating wave energy by friction (Burrows et al. 2005). The reduction of wave energy not only helps to reduce shoreline erosion, but also reduces vegetation loss by high energy waves, stabilizes sediments, and promotes the use of backwater systems by smaller animal and plant species that cannot handle the higher energy systems that would be present without the protection of the oyster reef (Meyer and Townsend 2000). The roughness of the reef, created by individual oysters protruding outward from the reef, creates a layer of turbulent mixing that supports nutrient cycling more than that of traditional breakwaters (Dame 1996).

Oysters filter organic phytoplankton from the water column as their primary food source, excreting inorganic matter into the water column, which is used by phytoplankton, creating a feedback loop that tends to short circuit the typical coastal ecosystem food web (Dame 1996). This feedback loop created by ecosystems typical of oyster reefs results in carbon, nitrogen, and phosphorous being processed at rates faster than typically found in coastal estuaries (Dame 1996).

2.2. TRADITIONAL BREAKWATER VS. ENGINEERED LIVING SHORELINE

Rock breakwaters seawalls are typically classified as hard or grey engineered structures and are not conducive to ecosystem growth and development. While these hard structures can be extremely effective at protecting the shoreline from wave energy and the erosion associated with it, their introduction can dampen the productivity of the surrounding ecosystem due to the loss of habitat conducive to the survival of a healthy ecosystem (Bozck and Burdick 2005). The introduction of living shorelines composed of naturally occurring animal shells, plants, and organic materials does just the opposite, benefitting the ecosystem by providing more usable habitat for fishery nurseries and improving productivity of the estuary (Manis et al. 2014).

Hard engineered shoreline protection structures are typically designed with a certain factor of safety, meaning they will be fully emerged at typical Mean High-Water levels, which allows them to fully dissipate day to day wave energies (Bodge 2003). This design is different from both natural oyster reefs and designed oyster reef like structures, which are typically both subtidal and intertidal, being fully submerged for some portion of the tidal cycle. Living shorelines, however, are designed in such a way to encourage the recruitment of oyster spat, which would promote three-dimensional growth as the structure transforms into a “living shoreline protection” (NOAA, 2017). As sea levels continuously rise, traditional breakwaters could be rendered ineffective with Mean Tide Levels eventually surpassing their design height, while living shoreline oyster reefs

will continue to grow through oyster reproduction allowing for greater longevity as a structure functioning to attenuate wave energy, while remaining intertidal to allow periodic transport of sediment into wetlands.

2.3. WAVE TRANSMISSION

Oyster reefs have been found to serve as a significant method of wave attenuation which can be quantified through the dimensionless wave transmission coefficient, K_t, calculated using the formula:

$$K_t = H_t / H_i \quad (1)$$

with H_t representing the transmitted wave height post attenuation through shoreline protection, and H_i representing the incident wave height prior to contact with the shoreline protection structure (Seelig et al. 1981).

By design, the tops of living shoreline structures tend to be lower to the water surface than traditional breakwaters, which can allow for runup and overtopping of the structure. Wave runup equation for wave transmission due to overtopping on smooth impermeable slopes is (Franzius 1965):

$$\boldsymbol{R = HC_1(0.123\frac{L}{H})^{(C_2\sqrt{\frac{H}{d}}+C_3)}} \quad (2)$$

where H is the mean wave height, L is the local wavelength, d is the water depth, and C_1, C_2, and C_3 are empirical coefficients, best represented by the following table (Seelig 1980).

Table 1. Empirical wave runup prediction coefficients for smooth impermeable slopes (Seelig 1980).

Front – face slope of breakwater	C_1	C_2	C_3
Vertical	0.958	0.228	0.0578
1 on 0.5	1.280	0.390	-0.091
1 on 1.0	1.469	0.346	-0.105
1 on 1.5	1.991	0.498	-0.185
1 on 2.25	1.811	0.469	-0.080
1 on 3.0	1.366	0.512	0.040

The calculated wave runup, *R*, is then used to determine the transmission caused by overtopping, K_{TO}, which is represented by the equation:

$$K_{TO} = \left(0.51 - \frac{0.11B}{h}\right)\left(1 - \frac{R_c}{R}\right) \quad (3)$$

where R_c is the structure crest freeboard, *R* is the previously calculated runup, *h* is the structure crest height, and *B* is the structure crest width (Seelig 1980). However as previously stated, this formula was developed for smooth, impermeable breakwaters, which living shoreline structures are not. By design, living shoreline structures are permeable and rough promoting a better ground for oyster colonization and higher use by aquatic species.

A few studies have gone into measuring wave transmission coefficients for low crested breakwaters (Allen et al., 2011, Van der Meer et al., 2005). The proposed formulas for the wave transmission coefficient for low crested breakwaters can be defined by:

$$K_t = -0.4\frac{R_c}{H_i} + 0.64\left(\frac{B}{H_i}\right)^{-0.31}\left(1 - e^{-0.5\xi}\right) \text{ for structures with } \frac{B}{H_i} < 10 \quad (4)$$

$$K_t = -0.35\frac{R_c}{H_i} + 0.51\left(\frac{B}{H_i}\right)^{-0.65}\left(1 - e^{-0.41\xi}\right) \text{ for structures with } \frac{B}{H_i} > 10 \quad (5)$$

which were derived by d'Angremond et al. (1996) and Van der Meer et al. (2005), respectively. In these formulas, ξ can be defined as the breaking parameter:

$$\xi = \frac{\tan\alpha}{S^{0.5}} \quad (6)$$

where α is the slope angle of the structure and S is the wave steepness (Van der Meer et al., 2005):

$$S = 2\pi \frac{H_i}{(gT_p^2)} \quad (7)$$

Van der Meer et al. (2005) went on to limit K_t to maximum and minimum values of:

$$K_{tu} = -0.006 \frac{B}{H_i} + 0.93 \quad (8)$$

$$K_{tl} = 0.05 \quad (9)$$

with K_{tu} and K_{tl} being the upper and lower wave transmission coefficients, respectively.

Research has been done to compare oyster shell bag breakwaters and other porous structures effects on wave transmission to that of a low crested breakwater mentioned above. Results from an experiment performed by Seabrook and Hall (2000) conclude that equations for low crested breakwaters does not adequately account for relative crest width and relative submergence for submerged rubble mound breakwaters. However, oyster shell bag breakwaters have been found to be realistically predicted by the equations above for low crested breakwaters (Allen et al., 2011, Van der Meer et al., 2005). It also has been found that strong correlations exist between wave transmission and simple dimensionless parameters for artificial reef breakwaters (Webb and Allen, 2015). Webb and Allen (2015) also noted that existing methodology for predicting wave transmission through rubble mound breakwaters did not provide as accurate of estimates for artificial reef breakwaters.

2.4. EFFECTS ON SEDIMENT TRANSPORT

An important factor in shoreline protection is the ability of the structure to allow water to flow, either by overtopping or physically passing through the permeable material. Traditional rock breakwaters form somewhat of an impermeable boundary between the offshore and nearshore environments, harming not only ecological functions, but also physical processes such as cross-shore sediment transport (National Academies Press, 2007). Cross-shore sediment

transport is the movement perpendicular to the shoreline that causes the natural phenomenon of the shoreward and seaward migration of dunes in coastal settings. Under normal circumstances, sediment is transported toward the coast from offshore, and vice versa for storm conditions (Pluijm et al., 1994). The conservation of sediment volume equation, given by National Academies Press (2007):

$$\frac{\partial h}{\partial t} = \frac{1}{\alpha}\left[\frac{\partial Q_x}{\partial x} + \frac{\partial Q_y}{\partial y}\right] + Q_s \quad (10)$$

where Q_x and Q_y are the sediment fluxes per width of flow in the x (cross-shore) and y (longshore) directions, respectively (National Academies Press, 2007). The term $\frac{\partial h}{\partial t}$ is the rate of change with water depth, a function of erosion or accretion, and alpha (α) representing the packing coefficient of the individual sediment grains as they settle. Q_s represents the sediment sources and sinks such as river inputs. Much of the Louisiana Gulf Coast now has been effectively cut off from the largest sediment source that it once had, the Mississippi River, so the Q_s term is less significant now than it historically has been.

The cross-shore transport term of the conservation of sediment volume equation also can be reduced when factoring in shoreline protection. Due to the nature of traditional shoreline protection measures, cross-shore transport for a given reach can be significantly impaired (National Academies Press, 2007). The transport of offshore sediment toward the shoreline takes place predominantly as bedload, which is blocked by traditional breakwaters (Pluijm et al., 1994). Studies have shown that under most circumstances, onshore sediment transport takes place as sheet flow (bed flow) that takes place in the bottom most portion of the water column (Mieras et al., 2017). Structures with solid bottoms will block shoreward sheet flow from reaching beyond the breakwater, cutting off a large portion of the cross-shore sediment supply. Studies show that

shoreline hardening can alter the traditional sediment flow and cause reduced sediment supply and a deeper nearshore region, often stranding sediment supply offshore of the structure (National Academies Press, 2007). Permeable structures allow water to flow through them, maintaining the hydrologic connectivity on shoreward and seaward sides of the structure which allows cross-shore sediment transport while still attenuating wave energy to enable sediment to fall out of suspension.

3. OBJECTIVES / METHODS

Living shorelines traditionally are judged on their ability to transmit waves, however that may not be the largest deciding factor in success. Larger permeabilities of the structures may allow for more cross-shore sediment transport, which may be the main source of sediment in protected marshes. The main objectives of this study are to analyze physical data to determine the effect of permeability and differences in wave transmission characteristics on subsequent shoreline retreat rates and volumetric change rates between different living shoreline alternatives across the Louisiana Gulf Coast. Currently, data exists on four living shoreline demonstrations completed by CPRA in Louisiana. The data collected includes offshore wave height, control inshore wave height, wave height immediately shoreward of the structure, peak wave periods, and water levels. The data will be analyzed in an attempt to answer the following:

1. Does porosity of a structure affect the erosion / accretion rates shoreward of the structure?
2. Do differences in wave transmission affect the erosion / accretion rates shoreward of the structure?
3. Does higher porosity of the structures negatively impact the wave transmission capabilities of the structure?

4. CALCULATIONS

4.1. POROSITY COEFFICIENT

For this study, a "Porosity Coefficient" was calculated for each structure in the four projects. In order to calculate a porosity coefficient, design reports or as-built reports were analyzed in order to accurately measure the structures used. Each shoreline protection structure was drawn to scale in AutoCAD 2018 in a long shore, two-dimensional cross section in order to calculate the surface area of the structure seaward face that would contribute to refracting water seaward instead of letting water pass through, $A_{Blocked}$. The cross-section area was calculated for each structure, and was subtracted from the total window area, A_{Total}, from seafloor to Mean Water Level at the structure, to calculate the unblocked area, $A_{Unblocked}$.

$$A_{Total} - A_{Blocked} = A_{Unblocked} \quad (11)$$

$A_{Unblocked}$ was then divided by A_{Total} to get the Porosity Coefficient, C_p, which for this purpose was considered to be similar to a permeability.

$$C_p = \frac{A_{Unblocked}}{A_{Total}} \quad (12)$$

Thus, structures with a higher C_p allow more water to freely pass through the shoreline protection structures, and subsequently structures with a lower C_p value allow less water to pass through. All porosity coefficients were calculated during this study for this study.

4.2. SOIL VOLUME CHANGE RATE

Over the four studies, the volumetric soil change rate was calculated in the units of:

$$(yards^3)(acre^{-1})(year^{-1}) \quad (13)$$

The middle 100 linear yards of each structure was analyzed to prevent any outside factors from skewing the actual performance of each structure, such as edge effects or impacts from adjacent structures. Each structure analyzed was longer than 100 yards. The differences in elevation survey transects from year to year were calculated and averaged over the 100 yards, giving the average

square yard of erosion or accretion per year for each structure (McGinnis 2017, McGinnis 2018). This was then multiplied by 100 yards to give the volume of change per year in:

$$(\boldsymbol{yards^3})(\boldsymbol{year^{-1}}) \quad \textbf{(14)}$$

By design, certain shoreline protection structures were constructed at different distances from the shoreline itself, creating variance in the above volumetric change rate calculation. In order to account for the differences in distance between the shoreline protection structure and the shoreline itself, individual polygons were created between the shoreline and the shoreline protection structure utilizing the same 100-yard section of structure calculated earlier. The rate calculated above was then divided by the area of this polygon (acres) in order to standardize the volumetric change rates across the different structures in the final equation of:

$$\boldsymbol{Soil\ Volume\ Change\ Rate} = (\boldsymbol{yards^3})(\boldsymbol{acre^{-1}})(\boldsymbol{year^{-1}}) \quad \textbf{(15)}$$

The soil volume change rate was calculated by CPRA for all project except for PO-0148, which was calculated for this study by the researcher. A reference image for a shoreline protection structure and its associated polygon can be seen in Appendix A.

4.3. WAVE TRANSMISSION

Wave information was collected for three of the four sites: LA-0016, PO-0148, and LA-0008. For all three of these sites, wave conditions were measured in 15-, 20-, or 30-minute bursts every hour at a frequency of 10-Hz. (Chauvin 2018, McGinnis 2017, McGinnis 2018). All wave transmissions used in this project were calculated by CPRA, with the exception of PO-0148, which was calculated by a T. Baker Smith employee (Chauvin 2018, McGinnis 2017, McGinnis 2018).

The measured parameters included significant wave height (H_s), peak wave period (T_p), and water level. Sampling periods with a significant wave height less than 0.5 feet were omitted due

to innate, local ripples forming behind the structures, not indicative of the wave transmission that took place.

From the collected data, a wave transmission coefficient, K_t, was calculated by:

$$K_t = \frac{H_t}{H_i} \quad (16)$$

For the projects, an offshore gauge was placed seaward of the structures to measure H_i, or incident wave heights prior to interaction with shoreline protection features. Inshore gauges were also placed shoreward of each structure to measure H_t, or transmitted wave heights prior to wave interaction with the shoreline protection features. The wave transmission coefficient was calculated to measure how effectively the shoreline protection feature was able to knock down wave energy and reduce wave heights as waves propagate toward the shore or marsh edge.

5. PROJECT MONITORING SUMMARIES

5.1. LA-0016

The LA-0016 Non-Rock Alternatives to Shoreline Protection project is located on the western side of Shark Island in Vermilion Bay, Iberia Parish (Figure 4). Four different shoreline protection methods were installed and monitored for efficiency and ability to attenuate wave energy. The four structures used in this project demonstrated four completely different methods of shoreline protection.

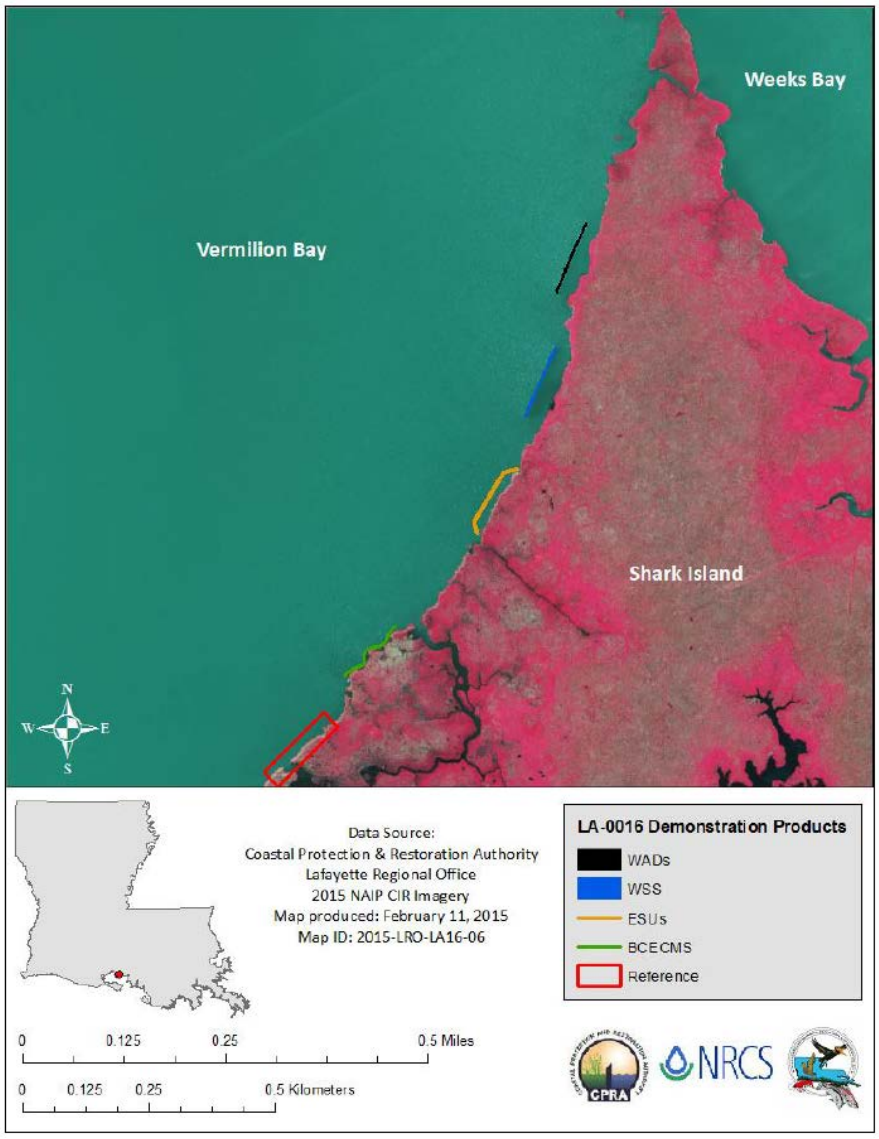

Figure 4. LA-0016 shoreline protection structures and reference locations (McGinnis, 2018)

The Wave Screen System (WSS, Figure 4) and the Wave Attenuation Devices (WAD®s, Figure 5) demonstrated two different types of structures each with open areas allowing water to pass through.

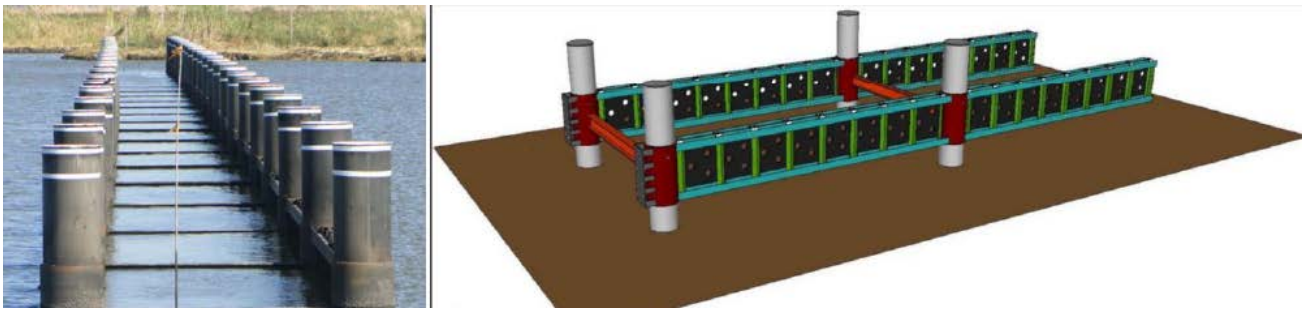

Figure 5. WSS installed in Vermilion Bay for LA-0016 (left) and WSS drawing (right) (McGinnis, 2018)

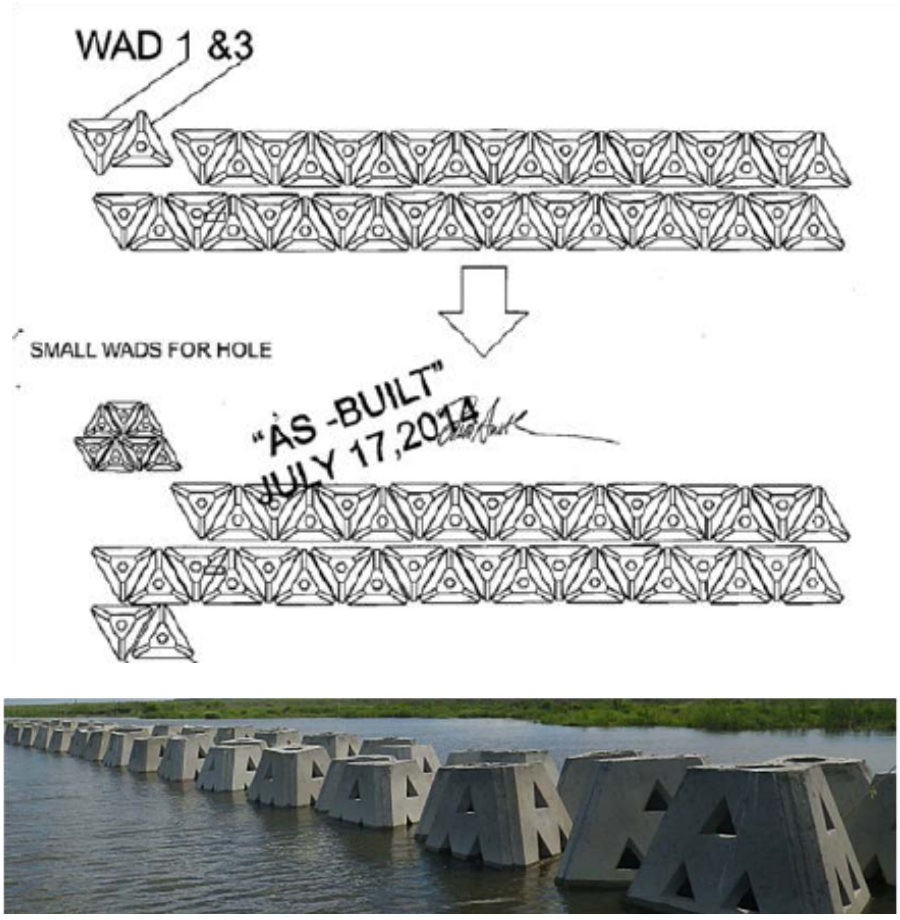

Figure 6. WAD®s As-Built Drawing (top) and WAD®s installed in Vermilion Bay (bottom) for LA-0016 (McGinnis 2018)

The EcoSystem Units (ESUs) are a shelf type structure thought to enhance oyster recruitment (Figure 7). The Buoyancy Compensated Erosion Control Modules (BCECMS) consist of a foam center cased in concrete to create a lightweight alternative to rock breakwaters (Figure 8). Both the ESUs and BCECMS demonstrated less open space than the WAD®s or WSS, similar to that of the traditional breakwater.

Figure 7. ESUs stacked before instilation and pile insertion (left) and ESUs installed in Vermilion Bay (right) for LA-0016 (McGinnis 2018)

Figure 8. Drawing of BCECMS (left) and installed BCECMS (right) in Vermilion Bay for LA-0016 (McGinnis 2018)

Cross sections were drawn for each of the four shoreline protection methods and the porosity coefficient was calculated and compared to the existing soil volumetric change rates and portrayed in Table 2.

Table 2. LA-0016 project monitoring summary and calculated Porosity Coefficient (C_p)

LA-0016				
Shoreline Protection Method	**Soil Volume Change Rate ($yd^3/ac/y$)**	**Shoreline Change Rate (ft/ y)**	**K_t (Waves greater than 0.5 ft)**	**Porosity Coefficient (C_p)**
WSS	576.20	-1.78	17.00	30.84%
WAD®s	217.90	-2.63	30.00	26.11%
ESUs	-38.20	-9.10	35.00	3.92%
BCECMS	-503.60	-5.89	19.00	0.00%
Reference	-2189.80	-51.15	N/A	N/A

As shown in Table 2, each shoreline protection method reduces down both the shoreline change rate and soil volume change rate relative to the reference area, which lost an alarming 51.15 feet of shoreline per year as well as 2,189.80 cubic yards per acre per year. All shoreline protection methods also had success attenuating wave energy as waves propagated through the structures.

5.2. PO-0148

The PO-0148 Living Shoreline Demonstration Project is located on the Eastern shore of Eloi Point in Eloi Bay located in the Pontchartrain Basin (Figure 9). Data collected on this demonstration captured four alternative methods of shoreline protection differing in shape and size, however two of the four are closely related. The two closely related structures are both Reef Ball products, hollow dome shaped structures installed in straight lines one after with multiple lines. Reef Ball Type 1 and Reef Ball Type 2 were both utilized in this project, differing in the amount of open area in the structure design (Figures 10 and 11).

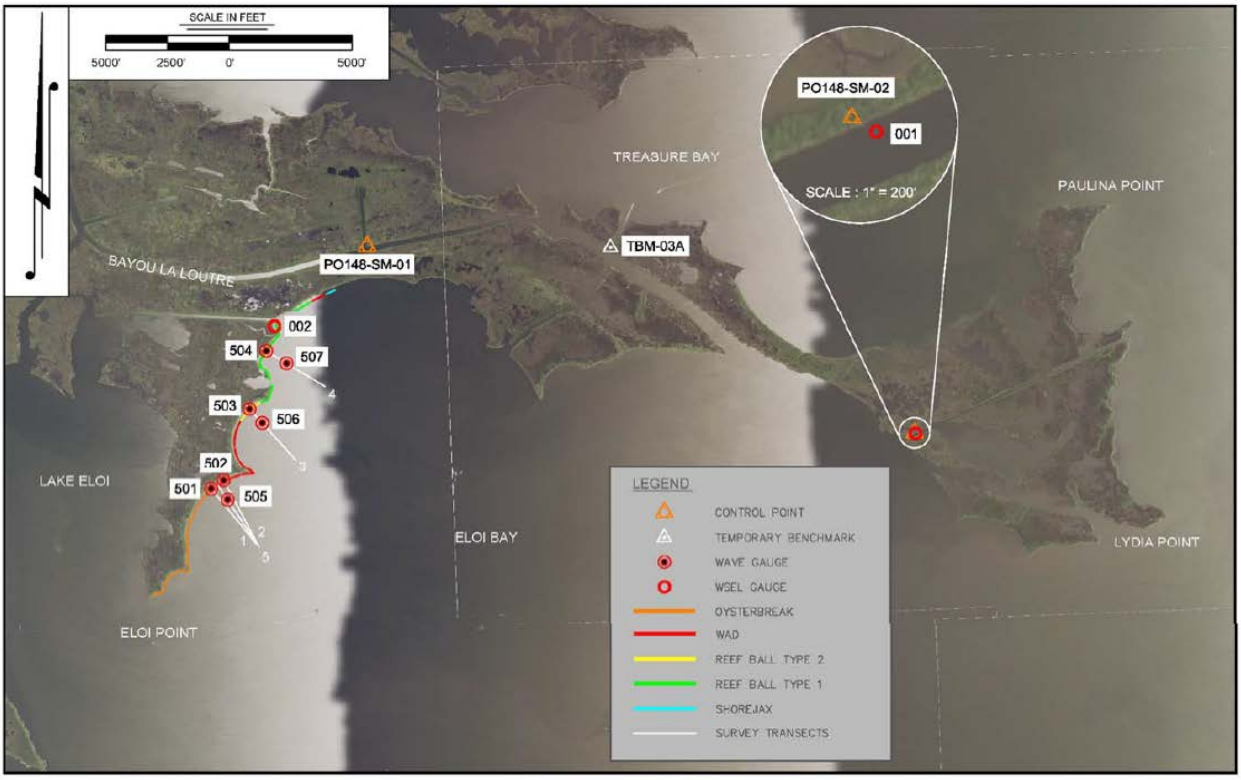

Figure 9. PO-0148 shoreline protection structures and reference locations (Chauvin, 2018)

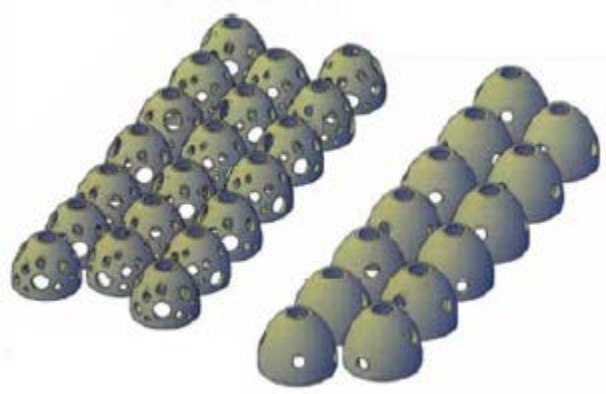

Figure 10. Reef Ball Type 1 (left) and 2 (right) conceptual drawings, (Coast and Harbor Engineering, 2015)

Figure 11. Reef Ball Type 2 (right) and 1 (left) deployed at PO-0148 project site (Chauvin, 2018)

Wave Attenuation Devices (WAD®s) were also used in this project similar to the WAD®s used in LA-0016, but with slightly different dimensions (Figure 12). The slight change in dimension and design of the WAD®s used in PO-0148 led to a slightly different porosity coefficient. The final shoreline protection method analyzed in this project was Oysterbreak™, a chain of hollow cylinders stacked one on top of another (Figure 13).

Figure 12. WAD®s installed at PO-0148 (left) and conceptual drawing of WAD®s used at PO-148 (Chauvin, 2018; Coast and Harbor Engineering, 2015)

Figure 13. OysterBreak™ installed at PO-0148 (left) and concpetual drawing of OysterBreak™ for PO-0148 (Chauvin, 2018; Coast and Harbor Engineering, 2015)

Cross sections were drawn for each of the four shoreline protection methods and the porosity coefficient was calculated and compared to the existing soil volumetric change rates and portrayed in Table 3.

Table 3. PO-0148 project monitoring summary and calculated Porosity Coefficient (C_p)

P0-0148					
Shoreline Protection Method	**Water Level**	**Rc/Hi**	**K_t Range**	**Porosity Coefficient (C_p)**	**Soil Volume Change Rate ($yd^3/ac/y$)**
OysterBreak™	-0.50	1.55	0.14 - 0.30	4.92%	-313.53
	1.00	0.05	0.37 - 0.60		
WAD®	-0.50	2.43	0.16 - 0.56	25.67%	265.77
	1.00	0.93	0.22 - 0.60		
Reef Ball Type 2	-0.50	2.28	0.15 - 0.60	15.77%	-666.50
	1.00	0.87	0.22 - 0.62		
Reef Ball Type 1	-0.50	1.7	0.11 - 0.34	33.83%	1164.50
	1.00	0.2	0.15 - 0.45		

All structures utilized in this project showed ability to attenuate wave energy, with each structure having a transmission coefficient ranging mostly below 0.5, meaning the transmitted wave height was reduced by fifty percent compared to the offshore incident wave height. The shoreline protection methods differed in success with soil volume change rate, with some having positive volume changes, or accretion, and others having negative calues for soil volume change rate, or erosion.

5.3. LA-0008

The LA-0008 Bio-Engineered Oyster Reef Demonstration Project was located on the northern shoreline of the Gulf of Mexico in the Mermentau Basin on the southern edge of the Rockefeller Wildlife Refuge east of Calcasieu Pass in Cameron Parish (Figure 14). The goals of this project were to assess a lighter Oysterbreak™ technology as an alternative to rock breakwaters. Oysterbreak™ was utilized due its lightweight design in comparison to traditional breakwaters. A lighter alternative was desired due to the extremely low soil load bearing capacity in the project area (McGinnis, 2017). Only two shoreline protection alternatives were used in this project, and both are Oysterbreak™ products. The only differences between the two are the concrete used to form the Oysterbreak™ rings and elevation. The western breakwater was made with Oysterkrete©, a lighter, less dense concrete designed to enhance oyster recruitment, and the eastern breakwater was made with Standard Weight Concrete (McGinnis, 2017) (Figure 15).

Figure 14. LA-0008 project location and reference area (McGinnis, 2017)

Figure 15. Oysterkrete© breakwater (top) and Standard Weight Oysterbreak™ aerial imagery from 2014 (McGinnis 2017)

The summary table for October of 2011 through August of 2016 is shown in Table 4. The two Oysterbreak™ structures have the same design and therefore have the same porosity coefficient. The gap noted in the table is the area between the two structures, which is more protected than the reference area due to sheltering provided by the adjacent Oysterbreak™ structures.

Table 4. LA-0008 project monitoring summary and calculated Porosity Coefficient (C_p)

LA-0008					
Shoreline Protection Method	**Soil Volume Change Rate ($yd^3/ac/y$)**	**Shoreline Change Rate (ft/y)**	***Kt* 2012**	***Kt* 2014**	**Porosity Coefficient (C_p)**
OBW (Oysterkrete©)	-937	-22 +- 1	0.49	0.3476	4.92%
OBE	-724	-23.0 +- 4.9	0.3316	0.1651	4.92%
Reference	-1266	-21.8 +- 6.2	0.7085	1.04	0%
Gap	-778	-25.3 +-1.0	N/A	N/A	0%

Both Oysterbreak™ West (OBW) and Oysterbreak™ East (OBE) proved to decrease the soil volume change rate with respect to the reference area. Both structures, however, showed to increase the shoreline change rate, meaning a negative impact on the shoreline behind the structures.

5.4. TE-0045

The TE-0045 Terrebonne Bay Shore Protection Demonstraition consists of three reaches of shoreline protection, two on the western shore of Lake Barre and one on the eastern shore of Lake Barre (Figure 16). Each of the three reaches contains three shoreline protection structures as well as a reference area. The Gabion Mat Treatment, one of the three methods used, consits of mesh bags filled with aggregate laid on the shoreline. This shoreline treatment, despite how effective it may or may not have been for erosion control, will not be analysed in this project as it is not a true living shoreline and does not allow for open area between the shoreline proteciton structure and the marsh edge.

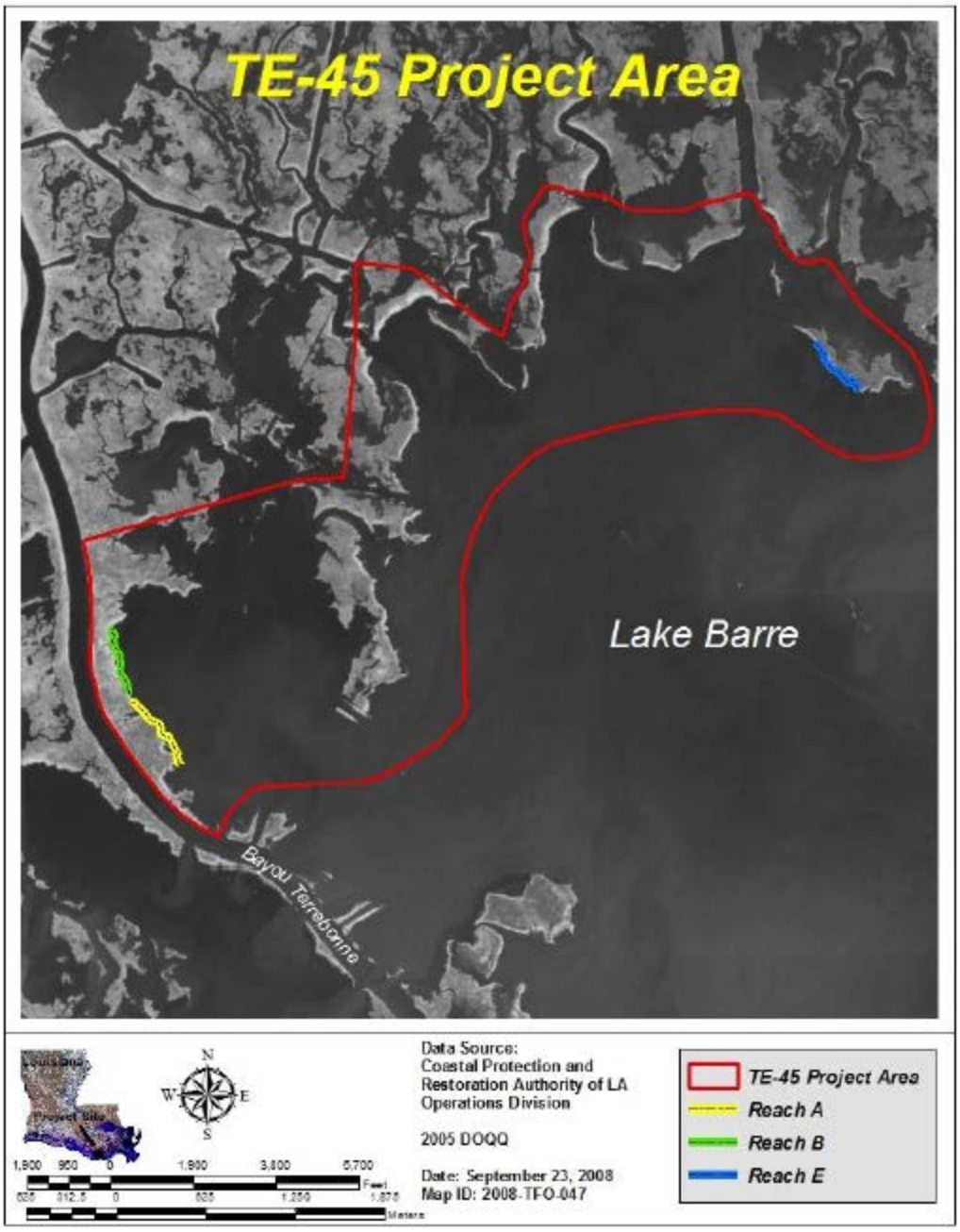

Figure 16. TE-0045 project location and reference area (Melancon et al. 2015)

The two other shoreline protection treatments used consist of A-Jack Treatments and ReefBLK treatments. The A-Jack treatment consisted of jack like structures interlocking with one another

for the span of the reach (Figure 17). The ReefBLK Treatments consisted of interlocking cages of oyster shells installed at a larger distance from the shoreline (Figure 18).

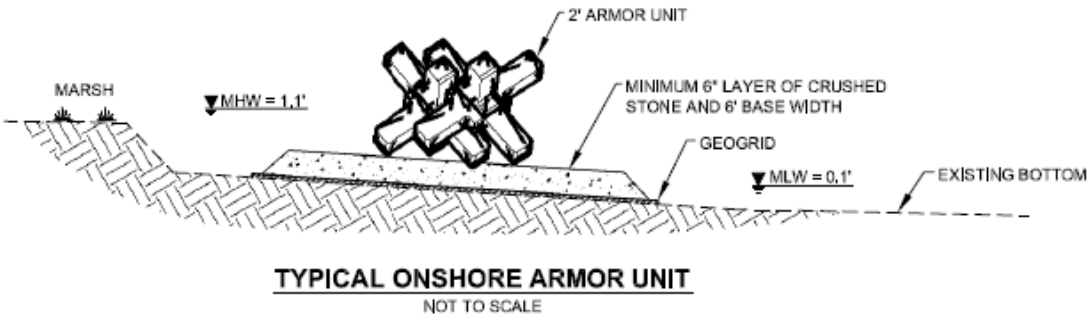

Figure 17. A-Jack Treatment at TE-0045 project site (top) and project completion report drawing of A-Jack Treatments (bottom) (Melancon et al. 2015; TBS Project Completion Report, 2008)

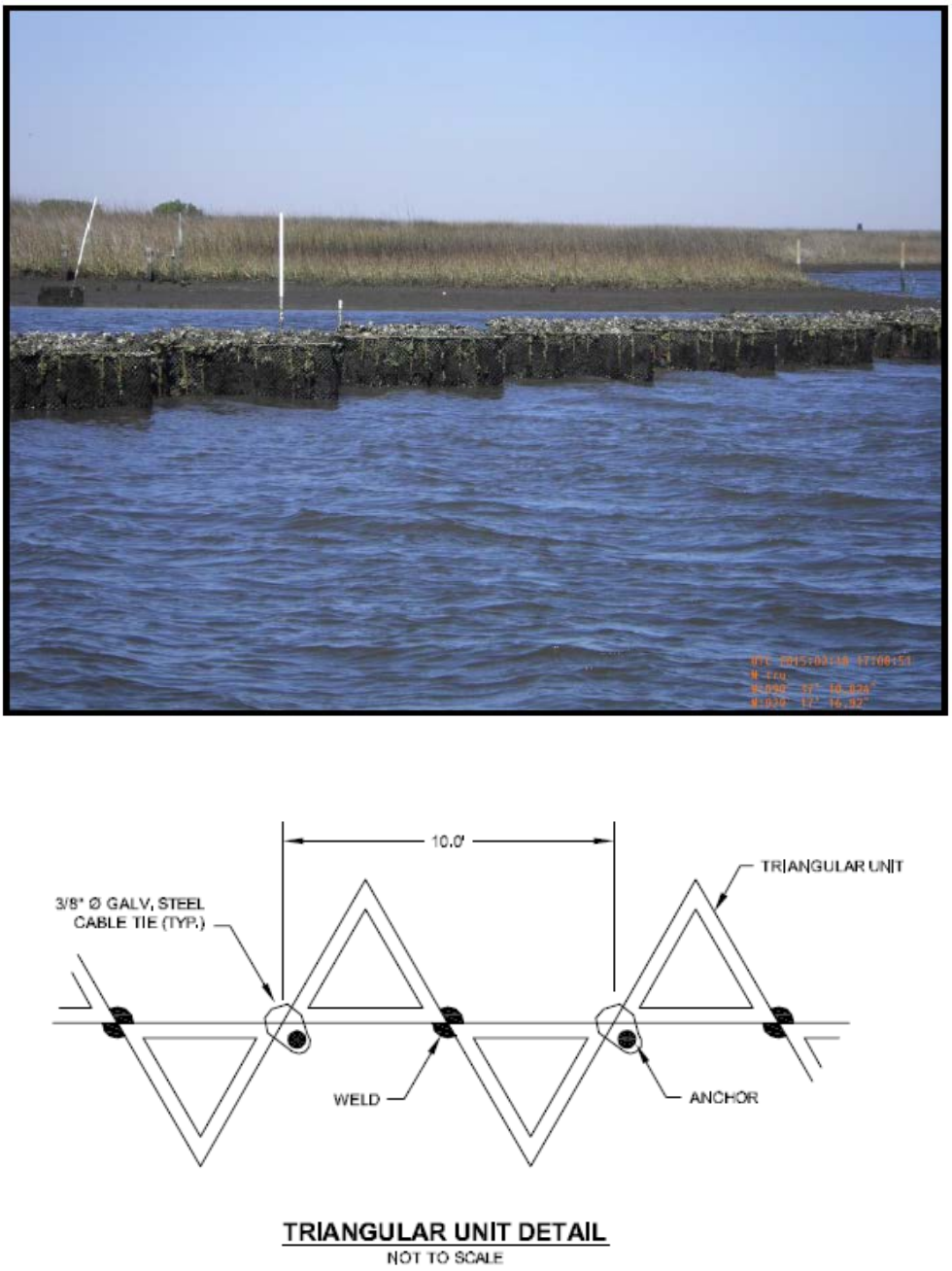

Figure 18. ReefBLKTreatment at TE-0045 project site (top) and project completion report drawing of ReefBLK Treatments (bottom) (Melancon et al. 2015; TBS Project Completion Report, 2008)

Each of the structures were tied into one another for the three Reaches, and data was collected for each reach. The focus of the TE-0045 project was on oyster colonization ability, and therefore

no wave data exists. However, soil volume change rate was collected, and can be compared to the calculated porosity coefficient (Table 5). No packing coefficient was provided for the ReefBLK shoreline protection treamtment, and a porosity coefficient of 35% was assummed similar to that of the packing coefficient of a lightweight aggregate.

Table 5. TE-0045 project monitoring summary and calculated Porosity Coefficient (C_p) for Reach A, Reach B, and Reach E

TE-0045		
Shoreline Protection Method (Reach)	**Soil Volume Change Rate ($yd^3/ac/y$)**	**Porosity Coefficient (C_p)**
A-Jack (A)	-70.73	13.52%
ReefBLK (A)	4.62	35%
Reference (A)	-107.01	0%
A-Jack (B)	-17.42	13.52%
ReefBLK (B)	1.43	35%
Reference (B)	-31.76	0%
A-Jack (E)	-68.83	13.52%
ReefBLK (E)	-19.51	35%
Reference (E)	-104.05	0%

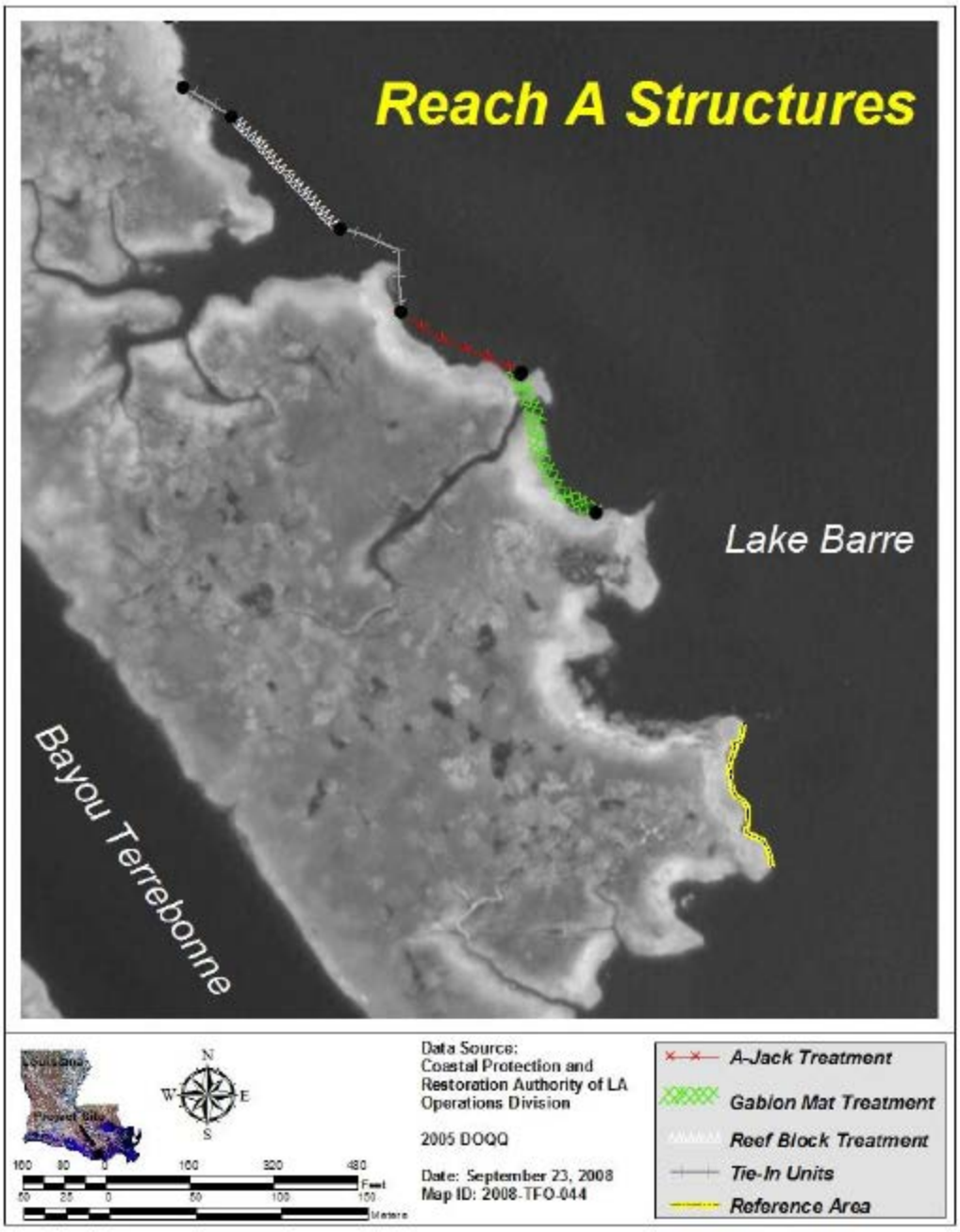

Figure 19. Reach A of TE-0045 structure location and reference area (Melancon et al. 2015)

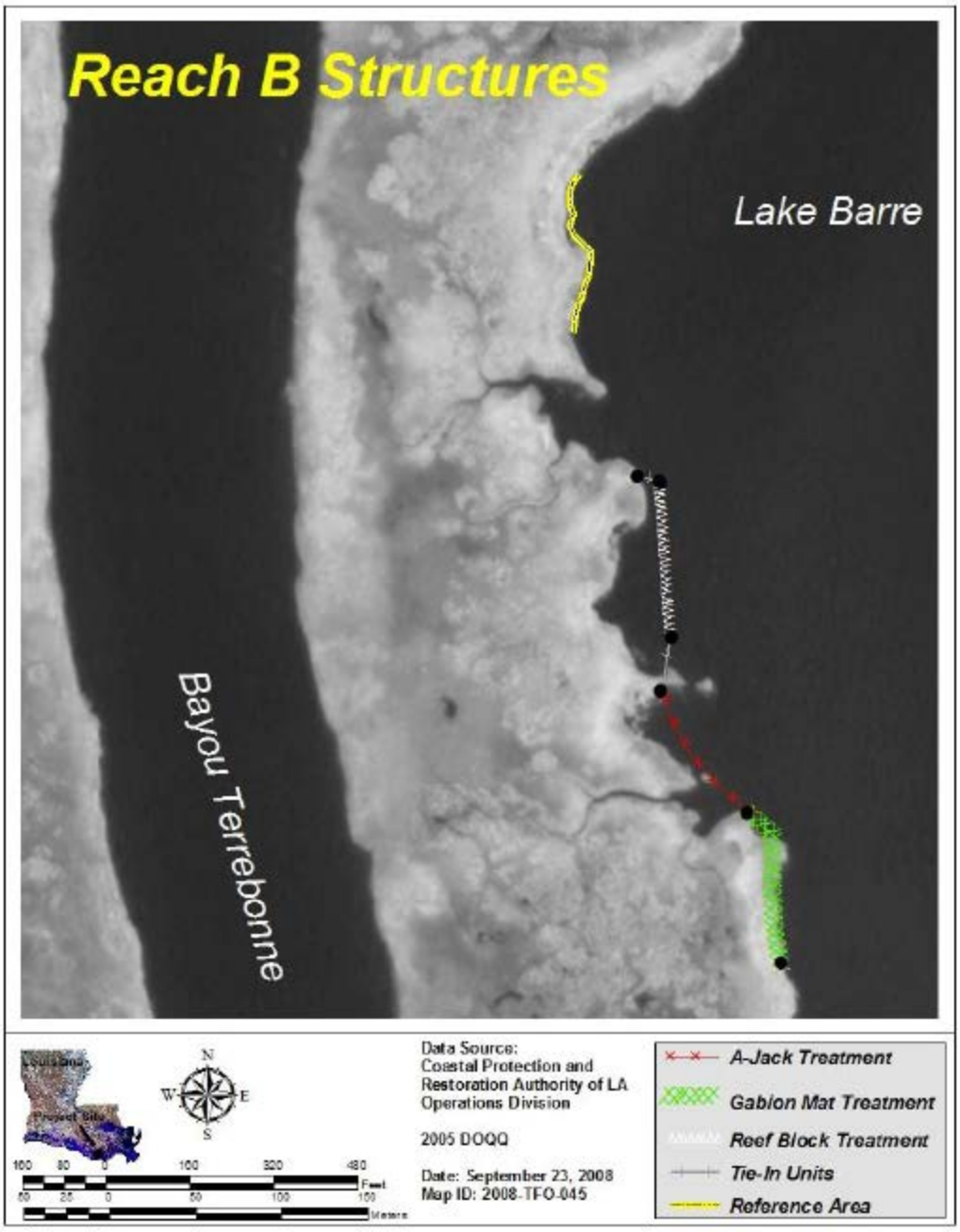

Figure 20. Reach B of TE-0045 structure location and reference area (Melancon et al. 2015)

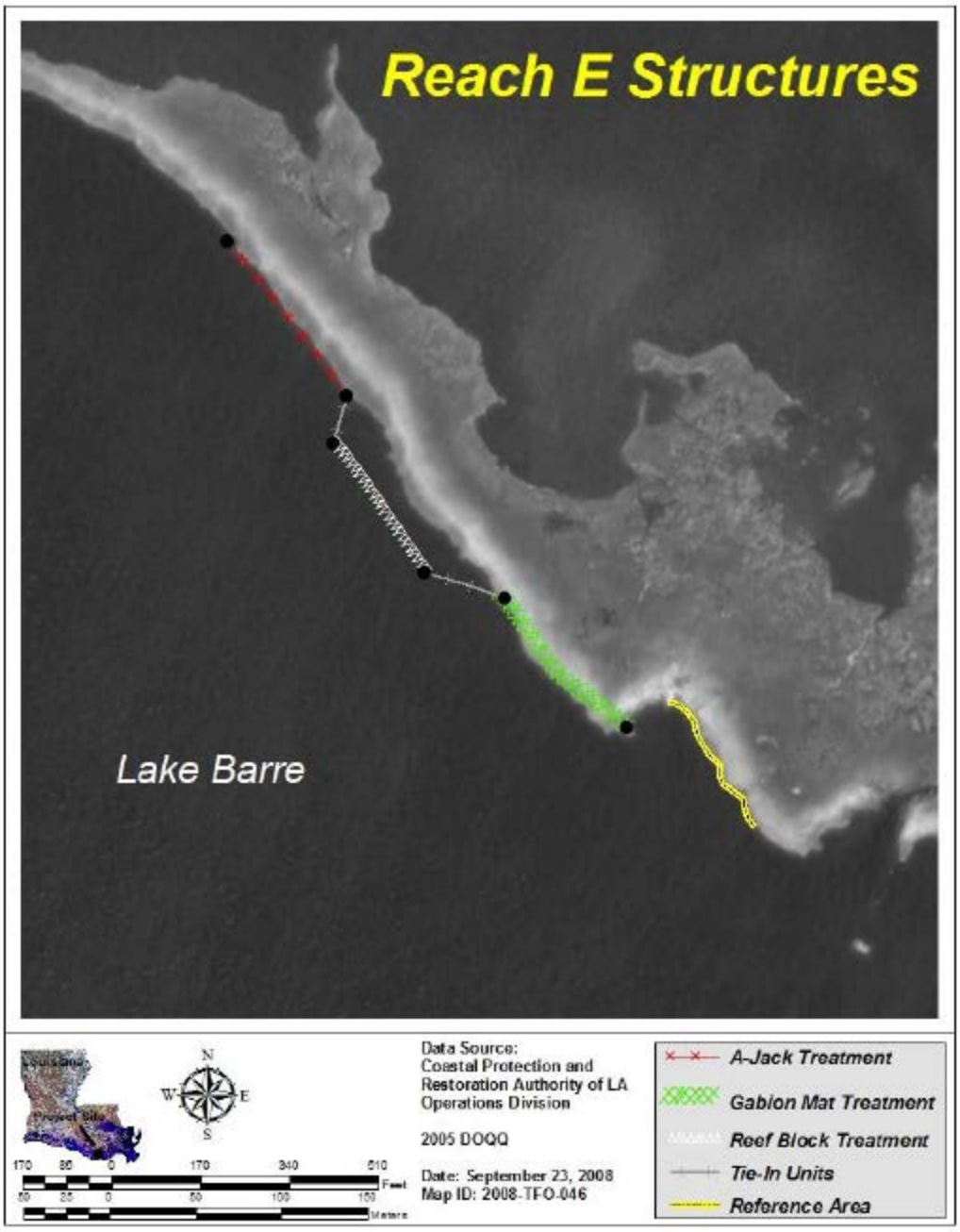

Figure 21. Reach E of TE-0045 structure location and reference area (Melancon et al. 2015)

6. RESULTS

6.1. POROSITY COEFFICIENT

A long shore, two-dimensional cross section was drawn for each of the shoreline protection structures at their most seaward face in AutoCAD 2018 utilizing the design specs or as-built drawings found on CPRA's CIMS Document Library Search. From these drawings, a porosity coefficient, C_p, was calculated and utilized to compare with the soil volume change rates for each project. Over the four projects, twelve porosity coefficients were compared, ranging from 0% (LA-0016, BCECMS) to 35% (TE-0045, ReefBLK). The porosity coefficients for each structure were graphed with their subsequent soil volume change rate to determine if a trend existed between the two.

Both the PO-0148 and LA-0016 projects had one strand of four structures, each with a different porosity coefficient. Graphs of the structure's porosity coefficient versus soil volume change rate for both projects show an increase in sediment retention with an increase in the porosity coefficient, meaning less of the two-dimensional cross section is blocked by the structure (Figures 22 and 23).

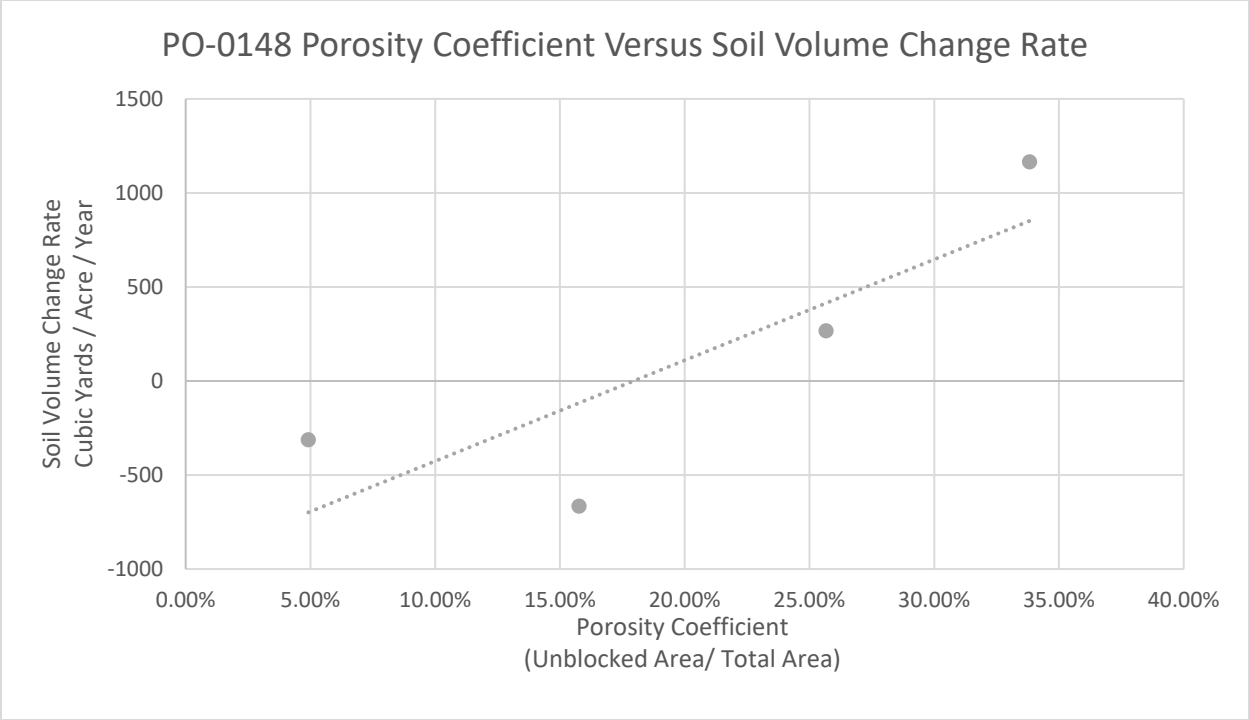

Figure 22. Porosity Coefficient versus Soil Volume Change Rate (yd^3 ac^{-1} yr^{-1}) for project PO-0148

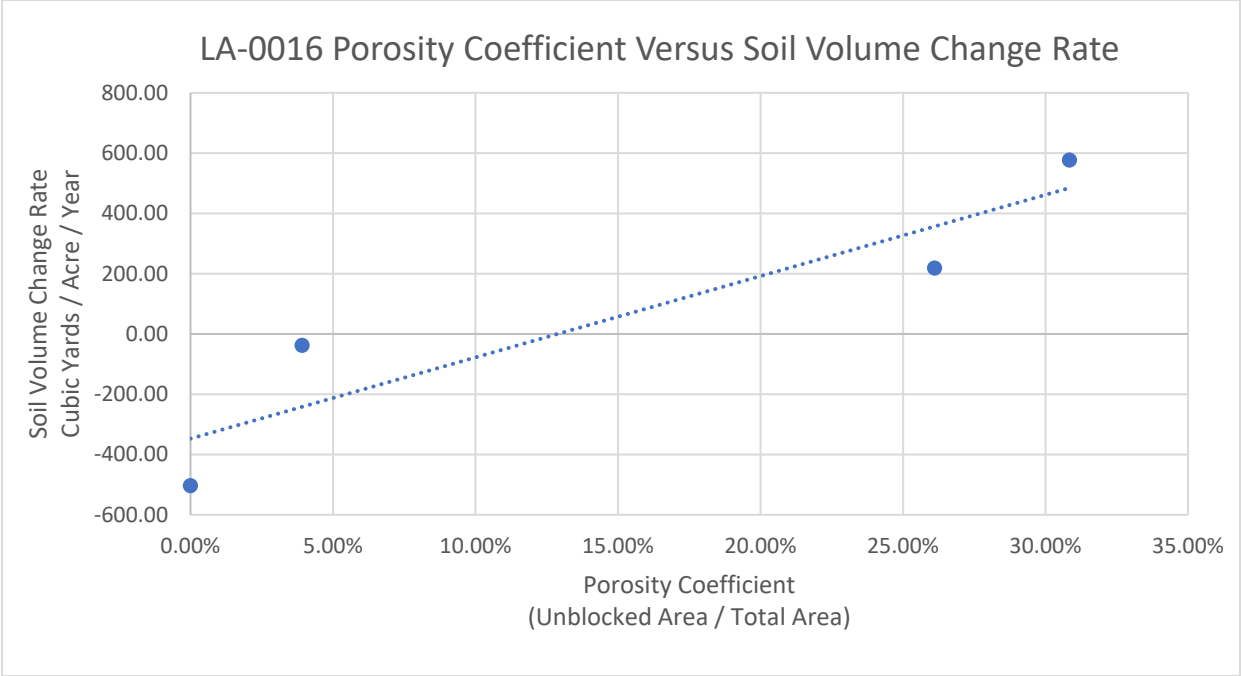

Figure 23. Porosity Coefficient versus Soil Volume Change Rate (yd^3 ac^{-1} yr^{-1}) for project LA-0016

The graph for project PO-0148 shows that the two structures with the lowest porosity coefficient show erosion over the monitoring period, while the two structures with the highest porosity coefficient gained volume in the monitored transects (Figure 22). The trendline developed for the PO-0148 project shows that the results are relatively linear with an R^2 value of 0.942. A similar trend was captured in the graph for the LA-0016 project (Figure 23). The two structures with the lowest porosity coefficients show erosion over the monitoring period, while the two structures with the highest porosity coefficient show accretion. The trendline developed for the LA-0016 project is also relatively linear, with an R^2 value of 0.8489. Both projects PO-0148 and LA-0016 demonstrate similarities of the positive effect of the structure's porosity coefficient to the increase in erosion prevention. The PO-0148 project did not have information regarding a reference area, and therefore it was not plotted on the Figure 18. The LA-0016 project did have a reference area monitored; however, it was not plotted on Figure 19 as it skewed the trendline because the soil volume change rate was drastically lower than that of all four structures at -2189.80 yds^3 ac^{-1} yr^{-1}. A logarithmic trendline could not be applied to attempt to include the reference area due to the negative values.

Project TE-0045 was slightly different in that it contains three reaches, each containing two structures and a reference site analyzed for soil volume change. The results for porosity coefficient versus soil volume change rate was plotted for each of the three reaches (Figure 24).

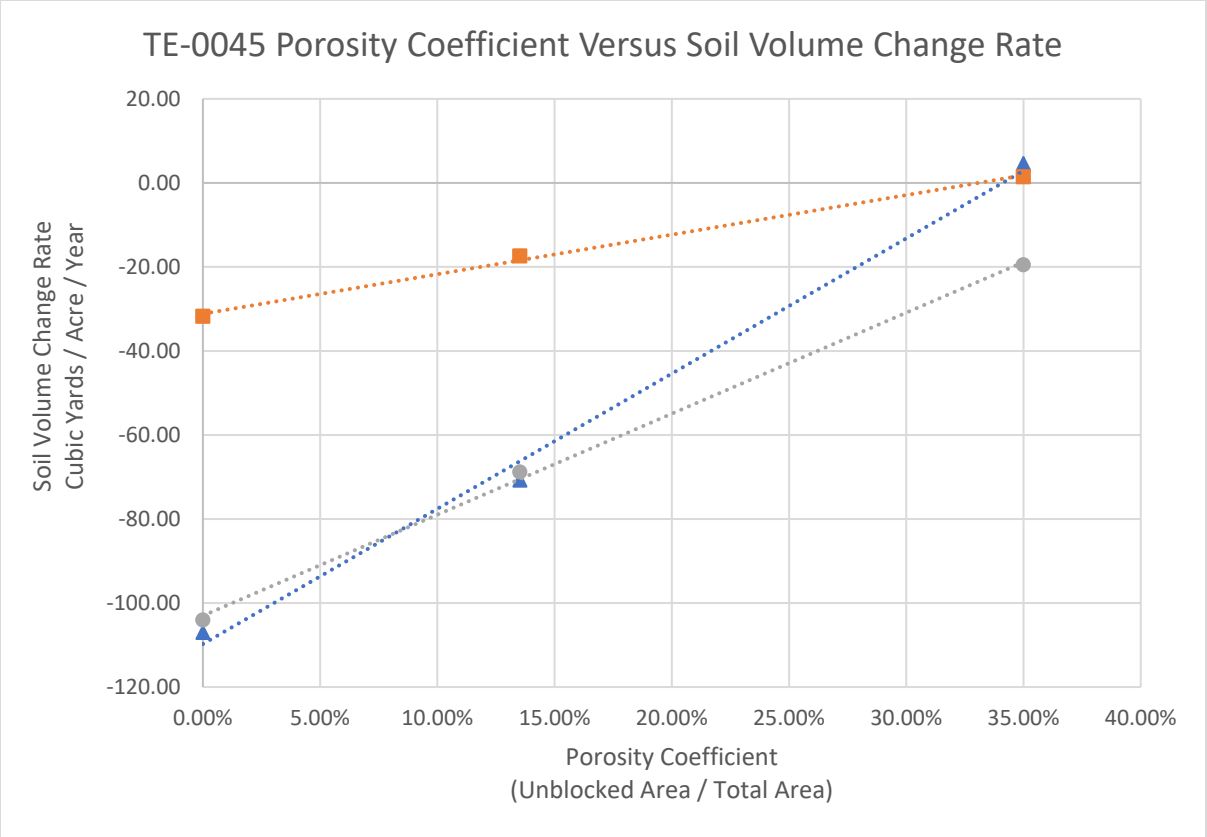

Figure 24. Porosity Coefficient versus Soil Volume Change Rate (yd^3 ac^{-1} yr^{-1}) for project TE-0045 Reach A (Blue Triangle), Reach B (Orange Square), and Reach E (Grey Circle)

As shown in Figure 20, both shoreline protection structures reduced the amount of erosion over the seven-year monitoring period relative to their associated reference areas (points with 0% porosity coefficient). The reference zones in Reaches A and B were not contiguous with other structures and were located approximately 135 and 105 yards away from the nearest shoreline protection structures, respectively. Reach E's reference area was located 30 yards away from the gabion mat units and set back so it was not contiguous with the shore face of the area protected by the mats. The closer proximity of the reference area to the gabion mat treatments is not concerning, as the mats did not induce wave breaking as they were laid on the shoreline. For all three reaches, the structure with the highest porosity coefficient showed to be most effective at reducing erosion,

and in even showed sediment accretion in Reach B and Reach E. The second shoreline protection structure registered a porosity coefficient of approximately half that of the other and was proven to also be effective at reducing erosion. The patterns developed over the graphs for all three reaches were extremely linear, showing an undeniable trend for the increase in free space for water to flow positively effecting the ability of the structure to reduce erosion.

Project LA-0008 only had two treatments deployed, each with the same porosity coefficient. The results for porosity coefficient versus soil volume change rate were plotted graphically to identify a trend (Figure 25).

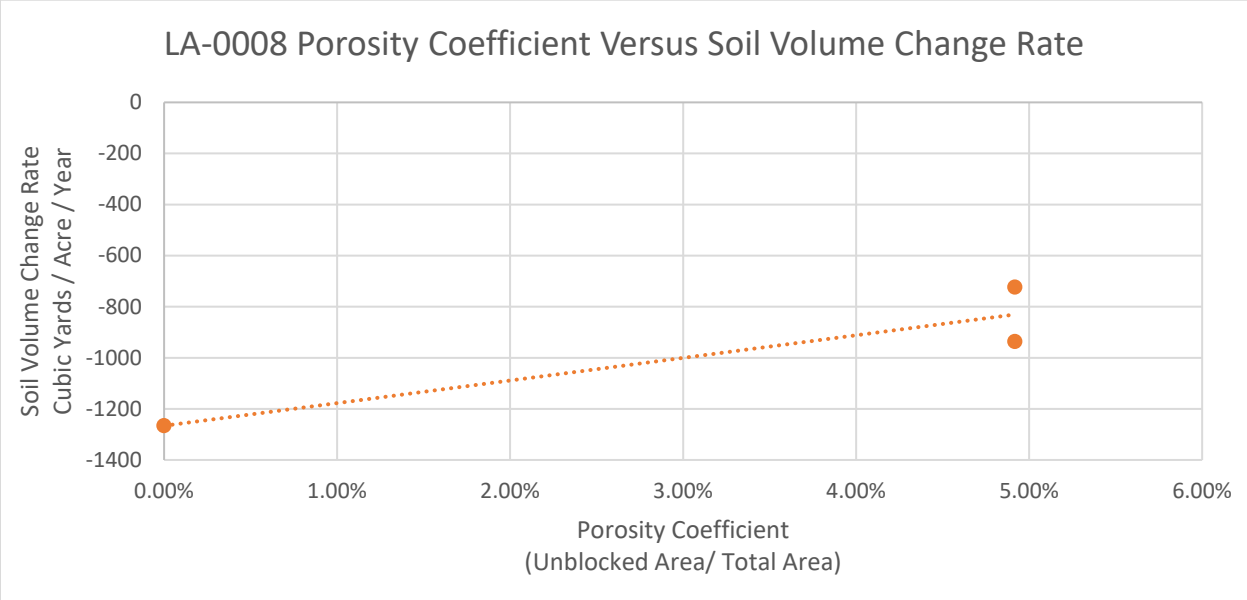

Figure 25. Porosity Coefficient versus Soil Volume Change Rate (yd^3 ac^{-1} yr^{-1}) for project LA-0008

This graph shows the positive effect each structure had when compared to the reference area, which is located approximately 700 yards away from the nearest shoreline protection structure. Due to the lack of diversity in the structures analyzed, the trendline developed for this project has little meaning other than showing that the structures helped to reduce erosion.

The transition point from erosion to accretion of sediment differs among the projects. The PO-0148 project graph shows a porosity coefficient of approximately 20.58% being the threshold for sediment accretion, while the LA-0016 project's threshold is slightly lower at a porosity coefficient of approximately 12.88%. Project TE-0045 showed even higher of a porosity coefficient needed for accretion, with all three Reaches showing a porosity coefficient of 30% or more would be needed to transition from erosion to accretion. The LA-0008 project did not have an actual transition point as both structures utilized still showed erosion during the monitoring period, however when extrapolated a porosity coefficient of approximately 14.30% would be needed for the transition of erosion to accretion.

Each of the structures used in all four projects were plotted together to see if an overarching trend could be seen despite the differences in site specific conditions associated with each site, such as sediment availability, wind and wave energy, soil characteristics, etc. (Figure 26).

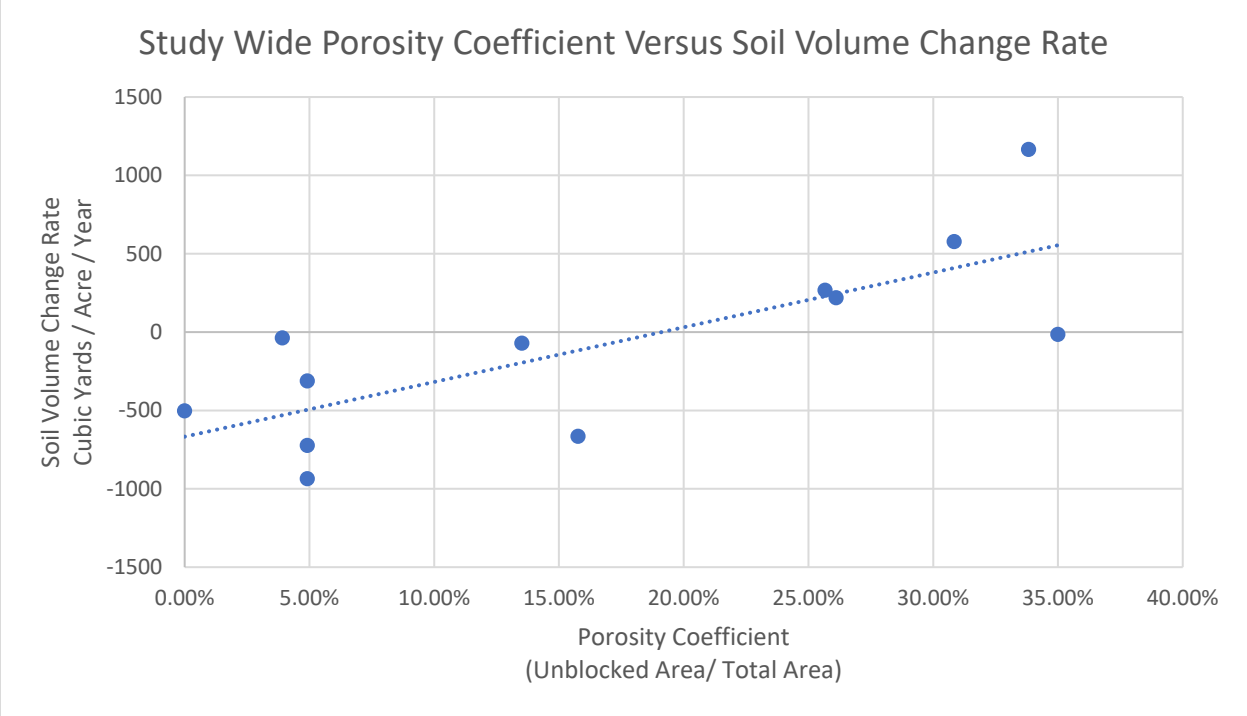

Figure 26. Study wide Porosity Coefficient versus Soil Volume Change Rate (yd^3 ac^{-1} yr^{-1}) for all structures

There are two general zones present in the study wide porosity coefficient versus soil volume change rate graph, one less than 10% porosity and one greater than 25% porosity. In general, the area of less than 10% porosity tended to show erosion, while the area of greater than 25% porosity generally shows accretion. Although the data does not fit the trendline quite as well, there is still a pattern of increased erosion prevention with an increase in a structure's porosity coefficient. A difference in results between the four projects should be expected, as the site conditions differ for each project. Structures similar in porosity coefficient are seen to have similar results of soil volume change rate, even when located at different project sites. Despite the different locations and conditions for each project site, there is a common overall theme that emphasizes the importance of hydrologic connectivity between the shoreward and seaward sides of a shoreline protection structure.

6.2. TRANSMISSION COEFFICIENT

The transmission coefficient calculated for projects PO-148, LA-0008, and LA-0016 were compared to the soil volume change rate to determine if a trend existed similar to the trend found involving a structure's porosity coefficient. Project TE-0045 was excluded from this discussion because no wave data was collected during the monitoring period. The average wave transmission coefficients for projects PO-0148, LA-0016, and LA-0008 were graphed versus the soil volume change rate similar to the previous section to see if a trend existed (Figures 27, 28, 29).

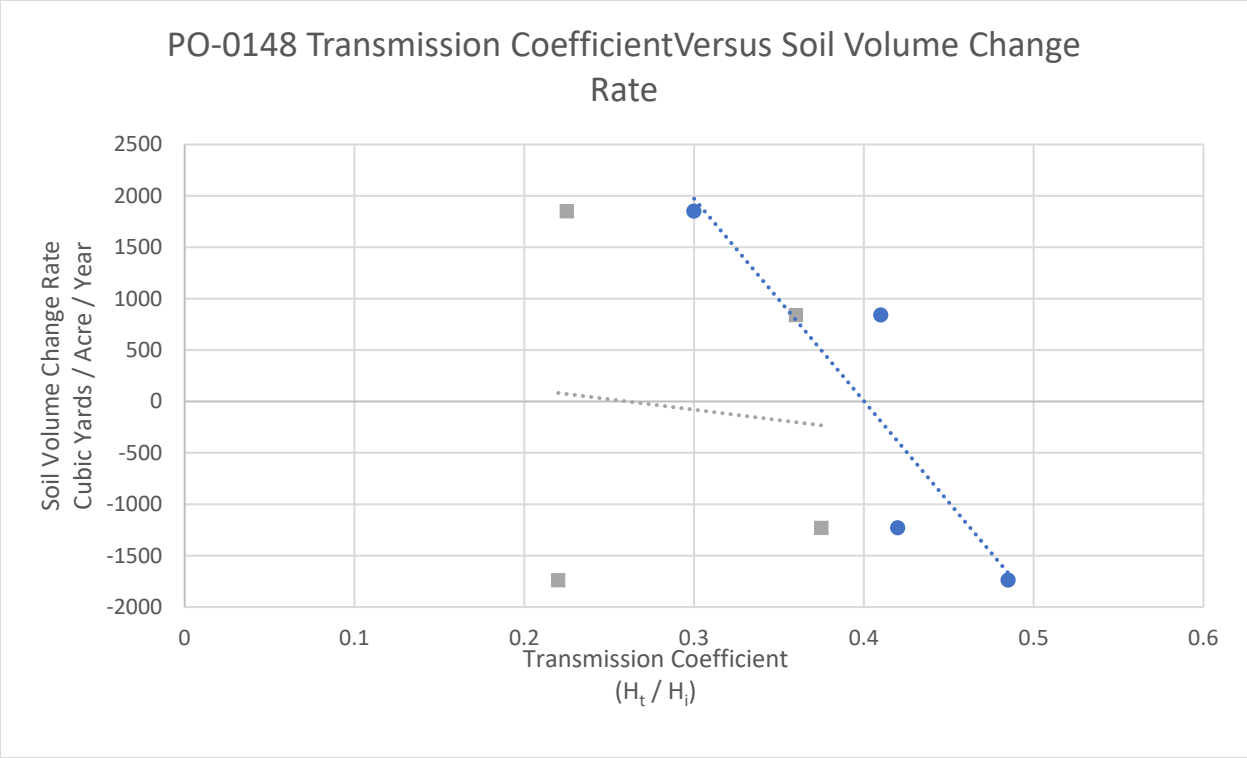

Figure 27. Transmission Coefficient versus Soil Volume Change Rate (yd^3 ac^{-1} yr^{-1}) for project PO-0148, Water level -0.5 (Grey Square) and Water Level 1.0 (Blue Circle)

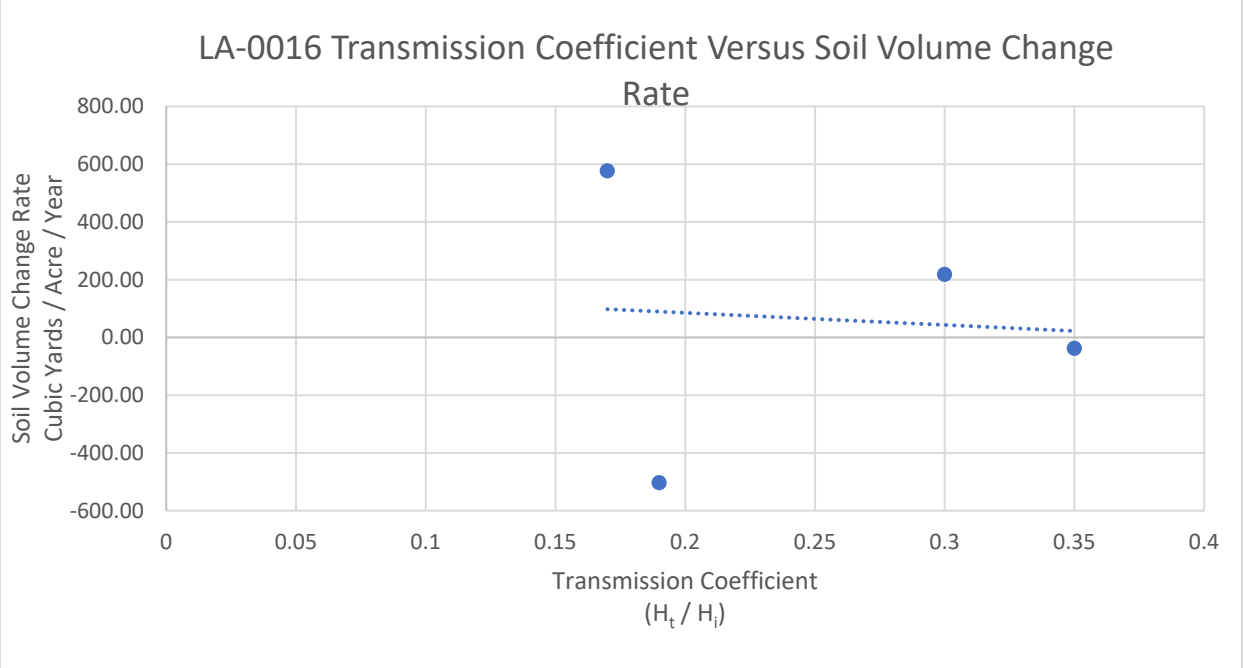

Figure 28. Transmission Coefficient versus Soil Volume Change Rate (yd^3 ac^{-1} yr^{-1}) for project LA-0016

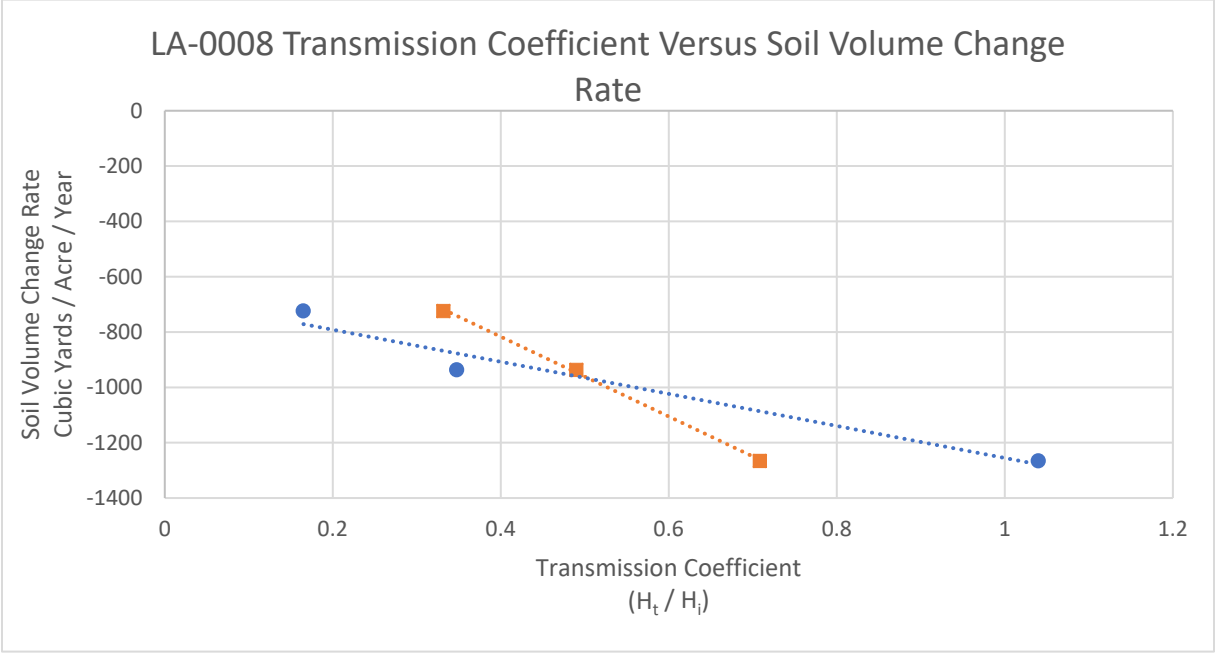

Figure 29. Transmission Coefficient versus Soil Volume Change Rate (yd^3 ac^{-1} yr^{-1}) for project LA-0008 for 2012 monitoring (Orange Square) and 2014 monitoring (Blue Circle)

All three projects show a decreasing trend in soil volume change rate with increasing wave transmission coefficient. Project PO-0148 had two monitored transmission coefficients, one for water levels of -0.5 feet (Grey trendline) and the other for water levels of 1.0-foot (Blue trendline) (Figure 27). The transmission coefficients for the -0.5 feet water level are in general lower than for the transmission coefficients related to the 1.0-foot water level, meaning that for lower water levels, more wave energy was dissipated, and transmitted wave heights were reduced. The trendline for the transmission coefficients was much more accurate for the 1.0-foot water level data when compared to the data for the lower water level, showing a much more linear effect.

The graph for the LA-0008 project also depicts two trendlines (Figure 29). The orange line represents the transmission coefficient for the 2012 monitoring period, and the blue line represents the transmission coefficient for the 2014 monitoring period. The results are near linear for both

years of monitoring, showing a strong trend of the effects of wave transmission on soil volume change rate. The data graphed for this project includes wave transmission and soil volume change rate for the reference area, located approximately 700 yards away from the nearest shoreline protection structure. The reference area for this project showed a transmission coefficient of 0.7085 in 2012, meaning wave heights decreased and wave energy was naturally dissipated as wave trains propagated shoreward, possibly due to wave breaking. However, this number increased to 1.04 in 2014, meaning wave heights increased in the same area where they once were breaking and decreasing. During this time period, the reference area was losing approximately 1,266 cubic yards per acre of sediment a year, leading to a deepening of the monitoring zone which could have decreased the depth limited wave breaking occurring in the previous monitoring period. Despite only having two structures involved in the study, the LA-0008 project shows a relationship between wave transmission and soil volume change rate.

The LA-0016 project shows much less of a relationship between wave transmission and soil volume change rate (Figure 28). Like projects PO-0148 and LA-0008, the best fit line for the LA-0016 project shows a decreasing trend in soil volume change rate with an increase in wave transmission coefficient, however the dataset is not linear. The findings from the LA-0016 monitoring summaries do not support a strong relationship between wave transmission and soil volume change rate.

The study wide graph for wave transmission coefficient versus soil volume change rate shows the same overall trend found in the three individual project graphs (Figure 30 and Figure 31). Figure 30 shows a linear trend line while Figure 31 shows a logarithmic trend. The data represented in both Figure 30 and Figure 31 fit their respective trends noticeably less than the study wide trend for porosity coefficient versus soil volume change rate. Some structures from different

projects that have similar transmission coefficients have vastly different soil volume change rates, whereas structures with similar porosity coefficients tended to have similar soil volume change rates.

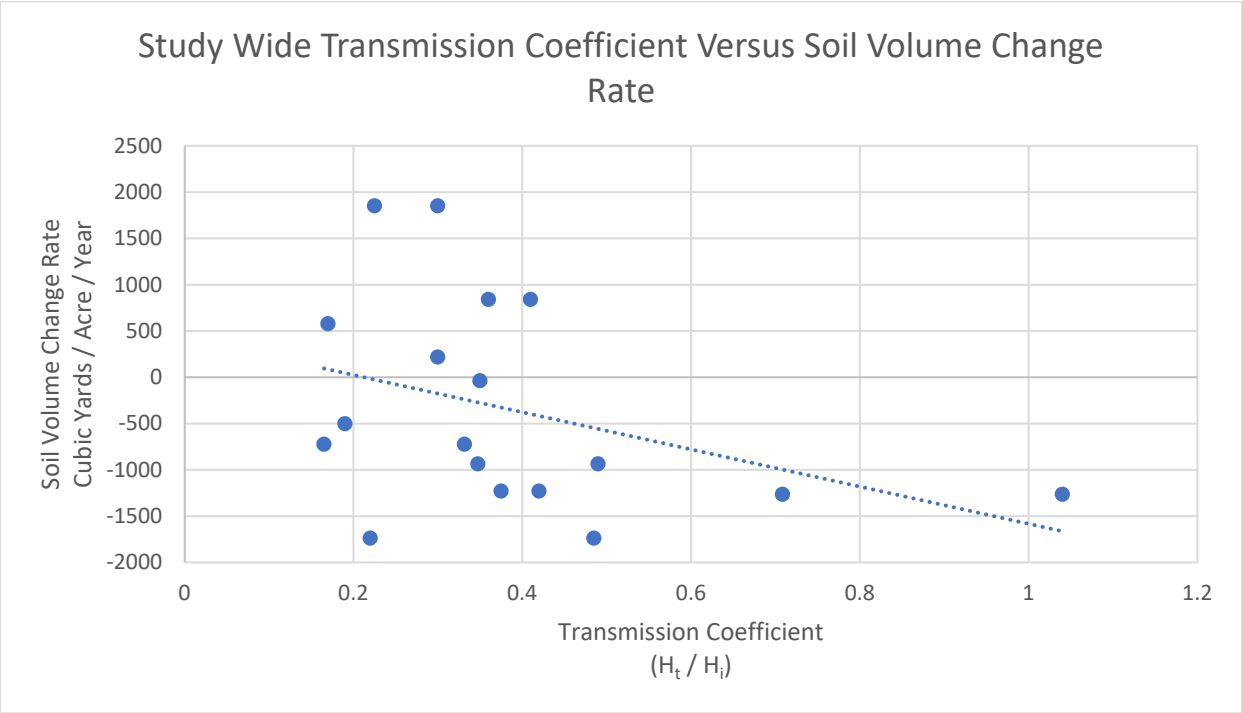

Figure 30. Study wide Transmission Coefficient versus Soil Volume Change Rate (yd^3 ac^{-1} yr^{-1}) for all structures

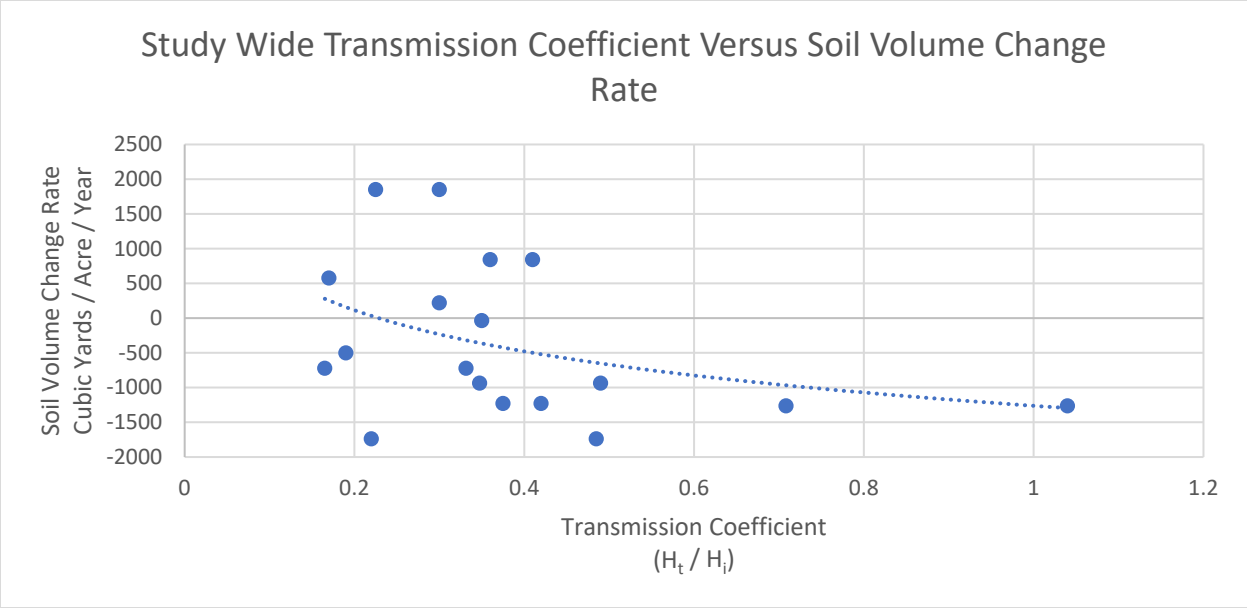

Figure 31. Study wide Transmission Coefficient versus Soil Volume Change Rate (yd^3 ac^{-1} yr^{-1}) for all structures (Logarithmic)

7. DISCUSSION

The calculated porosity coefficients were compared to the soil volume change rate results reported in the monitoring activities for each project. Overall, the porosity coefficient and soil volume change rate seemed to be correlated with one another, especially on a project by project case. While and linear relationship and pattern were still noticeable when plotting the study wide porosity coefficient versus soil volume change rate, the trend is not as clear the project specific porosity coefficient versus soil volume change rate graphs. The correlation is not quite as strong when all structures are graphed together, the positive trend still exists. The consistency of this trend implies that the positive retention of sediments is related to the amount of free space in each structure where water and sediment can move freely without being blocked by the structure. The wave transmission did not show as much of a correlation to the soil volume change rate as the porosity coefficient. There were some cases in which a noticeable pattern could be identified, and others where no pattern stood out. For LA-0016, the structure with the second lowest wave attenuation coefficient also produced the most negative soil volume change rate. The same structure also had the lowest porosity coefficient, meaning that in this case the large wave attenuation did not necessarily translate to success in stopping erosion. Overall, structures with more free area for water to flow, or a higher porosity coefficient, showed less erosion and in many cases even showed sediment accretion, while the wave transmission coefficient showed much less of an overall trend. This study assumes a constant porosity coefficient over time of the structure's deployment and monitoring events. This is most likely not the case, as some of the structures are designed for oyster recruitment, which could change the porosity values. Bioaccumulation of oyster spat will also change wave attenuation characteristics as well as the porosity coefficient, giving a variance in performance between monitoring events. Also, as the structures allow

sediment to flow through them, the sediment could possibly settle inside of the structure, blocking the area designated as porous in the original porosity coefficient calculations, which would also change the porosity coefficient over time.

The results for wave attenuation coefficient versus soil volume change rate was graphed with both a linear and logarithmic fit (Figures 30 and 31). The data from these graphs does not fit the trendline quite as well as the porosity coefficient versus soil volume change rate. This does not mean that wave transmission is not an important factor. All structures that possessed high porosity coefficients and positive soil volume change rates still showed the ability to attenuate wave energy. The fundamental role of both rock breakwaters and living shoreline protection features is to decrease the wave energy that impacts the marsh edge. This study places emphasis on the importance on the ability of a structure to not only attenuate wave energy and reduce wave heights, but also emphasizes the importance of a structure's ability to also allow water and sediment exchange between its shoreward and seaward sides.

Shoreline retreat rate was only calculated for two of the four projects. The results were negative for each structures shoreline retreat rate monitored. The structures in LA-0016 all showed a positive effect on the shoreline retreat rate, however all still showed erosion. Even when a structure showed a positive value for soil volume change rate, the shoreline retreat rate still showed a negative value (erosion) for all structures. It was decided to analyze the volumetric change rate in lieu of the shoreline retreat rate because a positive value in volumetric change rate indicates more success than a negative shoreline change rate would imply. It is also possible that the shoreline erosion could contribute to the positive values of soil volume change rate in the cases that had positive values.

The results of this study remain limited due to the differences between each project. Differences exist in the layout of the shoreline protection projects. The PO-0148 project shoreline protection structures are tied into one another with no gap between them (Figure 9). The three TE-0045 project reaches all utilized tie in units between the shoreline protection structures (Figures 19, 20 and 21). The LA-0016 and LA-0008 projects, however, have space between each of the structures, which could allow for more sediment transport into or out of the shoreward monitoring areas (Figures 4 and 14).

All projects were done at different times in different basins, with different objectives, goals, and methods. All projects studied had different results, which could largely be due to differences in the site-specific conditions. The PO-0148 project only has monitoring data collected for one-year post construction, while the TE-0045 project has seven years of monitoring recorded and reported in this project. The true effects of a shoreline protection project may not be able to be seen with only one year of data reported. Each project is in a different area of the Louisiana coast, which could cause a variation of data and outcomes. Each project location is subject to different wind and wave conditions due to the orientations of the project along the coast. The LA-0008 project is located along the northern coast of the Gulf of Mexico with miles of fetch to the south making it subject to uninterrupted waves from west southwest to east southeast. The LA-0016 project is located on the more protected eastern shore of Vermilion Bay with miles of fetch to the west, making it vulnerable to a narrower range of wave conditions. Reach E of the TE-0045 project is located on the northeastern shore of Grand Bayou Bourbeau and is susceptible to miles of open fetch to the south, while Reach A and Reach B of the TE-0045 project are even more protected, with less than one mile of fetch to the east. Project PO-0148 is subject to waves from the southeast with Eloi Bay opening into the Chandeleur Sound. The differences in location can also influence

the shoreline retreat rates for each project area. The exposed Rockefeller Refuge coast, where LA-0008 is located, has an extremely high shoreline change rate, averaging approximately -51 ft yr^{-1} over from 1995-2005 (Martinez et al. 2009). The project site for LA-0016 also has a high shoreline change rate of approximately -22.1 ft yr^{-1} from 1930s to 2005 (Martinez et al. 2009). The project area for TE-0045 has slightly less of a shoreline change rate of approximately -4.95 ft yr^{-1} from 1932-1983 (May and Britsch 1987). St. Eloi Bay, the location of the PO-0148 project, has the lowest shoreline change rate of approximately -1.0 ft yr^{-1} from 1956 to 2010 (Coast and Harbor Engineering, 2014)

According to Louisiana's Coastwide Reference Monitoring System (CRMS) the project areas have different marsh elevation change rates, meaning that the marsh surrounding each project area is either accreting sediment or subsiding/eroding at different rates, which could skew the project results relative to one another. For instance, CRMS Station 0589, near LA-0008 project site, reports a surface elevation change rate of -0.07 cm yr^{-1}, while stations close in proximity to LA-0016, TE-0045, and PO-0148 report surface elevation change rates of 0.72 cm yr^{-1}, 1.68 cm yr^{-1}, and 0.89 cm yr^{-1} respectively (CRMS0549, CRMS0355, and CRMS1024) (CRMS, Figure 26).

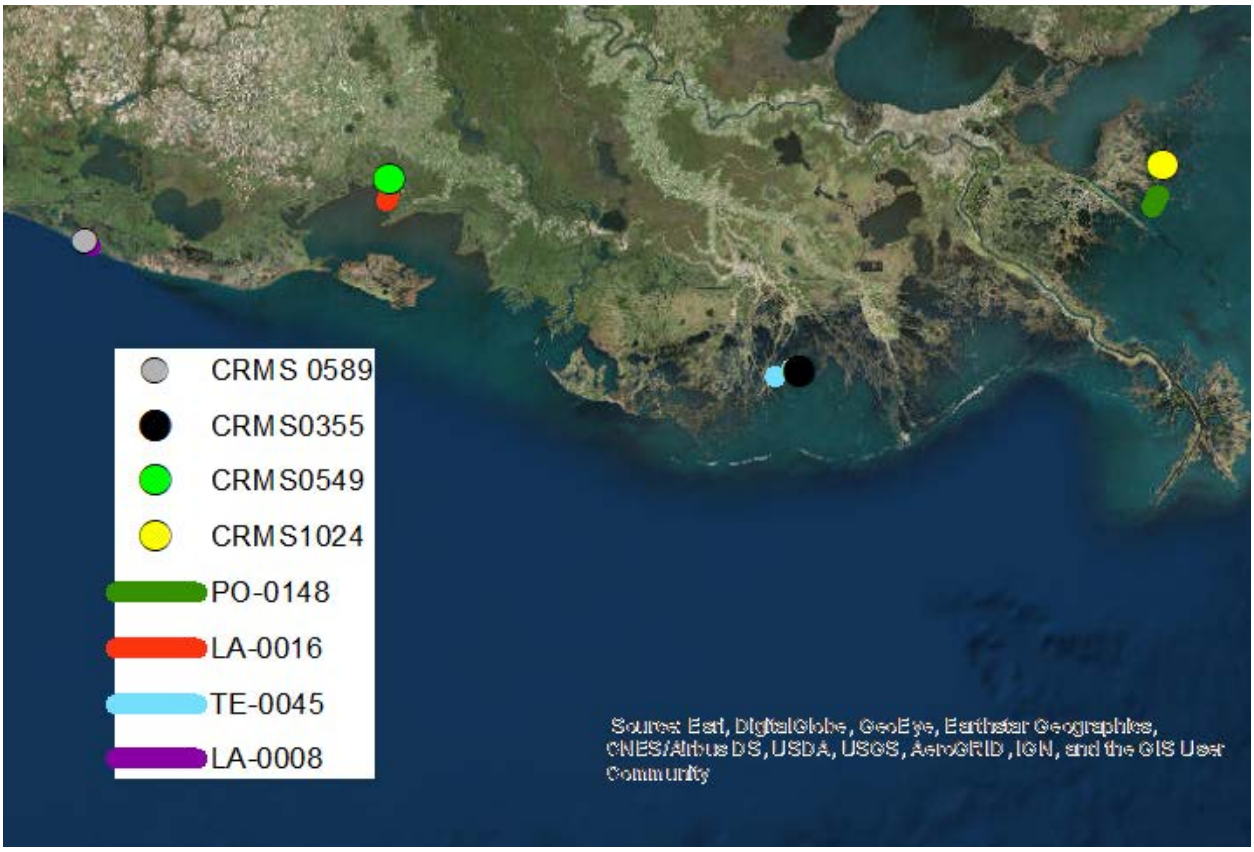

Figure 32. CRMS Monitoring Stations in relation to shoreline protection study sites

According to the same CRMS stations, a slight difference in bulk densities of existing sediment exists. Projects areas for LA-0016 and TE-0045 have the lightest of the four sediment supplies at 0.26833 g cm^{-3} and 0.28083 g cm^{-3} respectively, while project areas for LA-0008 and PO-0148 have heavier bulk densities measuring 0.34167 g cm^{-3} and 0.41833 g cm^{-3} respectively (CRMS0519, CRMS0355, CRMS0589, CRMS 0124). All of the differences noted above contribute to the variations seen in the outcomes of the different projects. Despite the differences in project designs, locations, and site-specific conditions, similarities in the trends associated with the monitoring data exist.

8. CONCLUSION

The results of this study provide a screening level insight into the complex processes surrounding coastal erosion and the continuing effort to combat it. Despite the limitations of the study and many differences between the projects, overarching trends were found that relate a structures permeability and wave transmission to soil volume change rate. Generalizations were made regarding the structures and the data collected on each. A structures wave transmission coefficient and porosity coefficient are constantly changing with the ebb and flood of tidal activity, and numbers were assigned for these values based on averages surrounding information available on Mean Tide Levels. The data analyzed in this project comes from outside sources, meaning differences in collection techniques may be present. This project in no way aimed to rank any of the living shoreline structures ahead of another but attempted to utilize multiple data sets to better understand the benefits of alternative methods to shoreline protection and their designs. Future work is recommended on the monitoring and maintenance/adaptive management of these projects and future projects. Overall, the data collected and reported by CPRA was consistent and helpful in the completion of this study. The monitoring and maintenance reports developed by CPRA provide a wealth of information and knowledge that should continue to be studied on an academic and professional level. A continuing analysis of all projects completed on the Louisiana coast is recommended for the further understanding and adaptive management of the projects used to combat coastal erosion.

While wave attenuation is an important factor in different shoreline protection designs, it is not the only thing to be concerned with. The data presented in this project brings to light the importance of the hydrologic connection between the seaward and shoreward water surrounding living shorelines and shoreline protection structures. Without enough area for water to flow and

tides to ebb and flood through a structure, stopping shoreline erosion could be difficult to achieve. Living shorelines should not isolate the shoreward waters between the structure and marsh edge from the surrounding waterbodies, as it could greatly reduce the sediment supply moving shoreward from open water. Wave attenuation is still a very important factor, as it helps to reduce energy in the shoreward areas of the system allowing for sediment to be deposited behind the structures. The right combination of permeability and ability to attenuate waves would allow for a greater project success rate and a healthier ecosystem. Further studies, monitoring, and data collection on existing projects could provide more insight into the proper balance between the two, as well as the other factors that influence the performance of living shoreline protection projects.

REFERENCES

Allen, Richard J., Webb, Brett M., 2011. "Determination of Wave Transmission Coefficients for Oyster Shell Bag Breakwaters" Coastal Engineering Practice: 684-697

Bodge, K. R., 2003. "Design Aspects of Groins and Jetties." In: Advances in coastal structure design. Ed. R. Mohan, O. Magoon, M. Pirrello. American Society of Civil Engineers (ASCE). Reston, VA. ISBN 0-7844-0689-8. Pp. 181-199

Boucher G., Boucher-Rodoni, R. 1988. In situ measurements of respiratory metabolism and nitrogen fluxes at the interface of oyster beds. *Mar. Ecol. Prog. Ser.* 44: 229-238.

Bozek CM, Burdick DM (2005) Impacts of seawalls on saltmarsh plant communities in the great Bay Estuary, New Hampshire USA. Wetl Ecol Manage 12(5):553-568

Buckley, M., Lowe, R. and Hansen, J., 2014. *Evaluation of nearshore wave models in steep reef environments*. Ocean Dynamics, 64(6): 847- 862

Burrows, Felicity, et al. "Restoration Monitoring of Oyster Reefs." *Science-Based Restoration Monitoring of Coastal Habitats: Volume Two*, 2005.

Coast and Harbor Engineering (2014). Living Shoreline Demonstration Project, Coastal Engineering and Alternatives Analysis. October 9, 2014.

Coast and Harbor Engineering (2015). Living Shoreline Demonstration Project, PO-148. Project Drawings. September 24, 2015.

Chauvin, Jason M., "Wave Attenuation by Constructed Oyster Reef Breakwaters" (2018). *LSU Master's Theses*. 4752. https://digitalcommons.lsu.edu/gradschool_theses/4752

CRMS, *Coastwide Reference Monitoring System*, https://lacoast.gov/crms_viewer/Map/CRMSViewer

Colden AM, Fall KA, Cartwright GM, Friedrichs CT (2016) Sediment suspension and deposition across restored oyster reefs of varying orientation to flow: implications for restoration. Estuar Coast 39:1435–1448

CPRA, 2017. "Coastal Protection And Restoration Authority." *Coastal Projects Map*, 2017, cims.coastal.louisiana.gov/outreach/OPL_Full_page.html.

CPRA. "Living Shoreline Demonstration Project (PO-148)." *Fact Sheet*

CRCL. *Oyster Shell Recycling*, www.crcl.org/programs/oyster-shell-recycling.html.

Davis, Jenny L. et al. "Living Shorelines: Coastal Resilience with a Blue Carbon Benefit." Ed. Bo Li. *PLoS ONE* 10.11 (2015): e0142595. *PMC*. Web. 24 Mar. 2018.

Demirbilek Z, Nwogu OG, Ward DL (2007) Laboratory Study of Wind Effect on Runup over Fringing Reefs, Report 1: Data Report. ERDC/CHL TR-07-4, Coastal and Hydraulics Laboratory

Louisiana Coastal Protection and Restoration Authority. Louisiana's Comprehensive Master Plan for a Sustainable Coast (2017). Retrieved from: http://coastal.la.gov/wp-content/uploads/2017/04/2017-Coastal-Master-Plan_Web-Book_CFinal-with-Effective-Date-06092017.pdf

Martinez, L., S. O'Brien, M. Bethel, S. Penland, and M. Kulp. 2009. Louisiana Barrier Island Comprehensive Monitoring Program (BICM), Volume 2: Shoreline Changes and Barrier Island Land Loss 1800s-2005. University of New Orleans, Pontchartrain Institute for Environmental Sciences, New Orleans, LA. 32 pp.

Manis, J.E.; Garvis, S.K.; Jachec, S.M.; Walters, L.J. Wave attenuation experiments over living shorelines over time: A wave tank study to assess recreational boating pressures. J. Coast. Conserv. 2015,19, 1–11.

May, J. R. and L. D. Britsch. 1987. Geological Investigation of the Mississippi River Deltaic Plain: Land Loss and Land Accretion. Techical Report GL-87-13. U.S. Army Engineer District, New Orleans. New Orleans, Louisiana.

McGinnis, II, T. E. 2017. *2017 Operations, Maintenance, and Monitoring Report for Bioengineered Oyster Reef Demonstration Project (LA-0008): Final Closeout Report. Coastal Protection and Restoration Authority of Louisiana; Lafayette, Louisiana.* 44 pp and Appendices.

McGinnis, II, T. E. 2018. *2018 Operations, Maintenance, and Monitoring Report for Non-rock Alternatives to Shoreline Protection Demonstration Project (LA-0016): Final Closeout Report.* Coastal Protection and Restoration Authority of Louisiana; Lafayette, Louisiana. 41 pp plus Appendices.

McGlathery KJ, Reynolds LK, Cole LW, Orth RJ, Marion SR, Schwarzschild A (2012) Recovery trajectories during state change from bare sediment to eelgrass dominance. Mar Ecol Prog Ser 448:209-221. https://doi.org/10.3354/meps09574

Melancon, E. J. Jr., G. P. Curole, B. J. Babin, and Q. C. Fontenot. 2015. *2015 Operations, Maintenance, and Monitoring Report for Terrebonne Bay Shore Protection Demonstration (TE-45), Coastal Protection and Restoration Authority of Louisiana, Thibodaux, Louisiana. 97 pp. and Appendices.*

Meyer, D.L. and E.C. Townsend. 2000. Faunal utilization of created intertidal eastern oyster (*Crassostrea virginica*) reefs in the southeastern United States. *Estuaries* 23: 34-45

Mieras, R., Puleo, J. A., Anderson, D., Cox, D. T., and Hsu, T. -J., 2017. Large-scale experimental observations of wave-induced sediment transport over a surf zone sandbar, Proc. 18th Int. Conf. Coast. Dyn., Helsingør, Denmark

National Academies Press. 2007. *Mitigating shore erosion along sheltered coasts*. (2007). Washington, D.C.: Committee on Mitigating Shore Erosion Along Sheltered Coasts. Doi:https://www.nap.edu/read/11764

Nederhoff, C.M., et al. "Modeling the Effects of Hard Structures on Dune Erosion and Overwash." 2015, doi:10.1142/9789814689977_0219.

Nelson K. A, Leonard L. A., Posey M. H., Alphin T. D., and Mallin M. A. 2004. Using transplanted oyster (*Crassostrea virginica*) beds to improve water quality in small tidal creeks: A pilot study. *J. Exp. Mar. Biol. Ecol*. 298: 347–368.

NOAA. "Living Shorelines." *NOAA Fisheries*, www.fisheries.noaa.gov/insight/living-shorelines.

Pluijm, M., van der Lem, J.C., Kraak, A.W., de Ruig, J.H.W, 1994. Offshore breakwaters versus beach nourishments, a comparison, Coastal Engineering Journal, Chapter 231: 3208-3222

Pomeroy, A., Lowe, RJ., Symonds, G., Van Dongeren, A.R., and Moore, C., 2012. The dynamics of infragravity wave transformation over a fringing reef, *Journal of Geophysical Research*, 117(C11022).

Puglisi, Melany P., 2008, *Crassostrea Virginica* "Smithsonian Marine Station at Fort Pierce." www.sms.si.edu/irlspec/Crassostrea_virginica.htm.

Quataert, E., Storlazzi, C.D., Rooijen, A., Cheriton, O.M., and Dongeren, A., 2015. The influence of coral reefs and climate change on wave-driven flooding of tropical coastlines. *Geophysical Research Letters*, 42:6407-6415

Reidenbach, Matthew A., Berg, Peter, Hume, Andrew, Hansen, Jennifer C. R., Whitman, Elizabeth R., (2013), Hydrodynamics of intertidal oyster reefs: The influence of boundary layer flow processes on sediment and oxygen exchange. *Limnology and Oceanography: Fluids and Environments*, 3, 10.1215/21573689-2395266.

Riisgard HU. 1988. Efficiency of particle retention and filtration rate in 6 species of Northeast American bivalves. Marine Ecology Progress Series 45:217-223.

Roelvink, D., et al. (2009). "Modelling storm impacts on beaches, dunes and barrier islands." Coastal Engineering 56(11-12): 1133-1152.

Schulte, D., G. Ray, and D. Shafer. 2009. Use of alternative materials for oyster reef construction. EMRRP Technical Notes Collection (ERDC TN-EMRRP-ER12). Vicksburg, MS: U.S. Army Engineer Research and Development Center.

Scyphers, Steven B. et al. “Oyster Reefs as Natural Breakwaters Mitigate Shoreline Loss and Facilitate Fisheries.” Ed. Howard Browman. *PLoS ONE* 6.8 (2011): e22396. *PMC*. Web. 24 Mar. 2018.

Seabrook, Stuart R.; Hall, Kevin R.. WAVE TRANSMISSION AT SUBMERGED RUBBLEMOUND BREAKWATERS. Coastal Engineering Proceedings, [S.l.], n. 26, jan. 1998. ISSN 2156-1028. Available at: https://journals.tdl.org/icce/index.php/icce/article/view/5740>. Date accessed: 08 May 2019. doi:https://doi.org/10.9753/icce.v26.%p.

Seelig, William N., 1979. “Estimation of Wave Transmission Coefficients for Permeable Breakwaters.” CETA 79-6, USACE, CERC, Fort Belvoir, Va.

Seelig, William N., Ahrens, John P., 1981. “Estimation of Wave Reflection and Energy Dissipation Coefficients for Beaches, Revetments, and Breakwaters.” TP 81-1, USACE, CERC, Fort Belvoir, Va.

Seelig, William N., 1980. “Two-Dimensional Tests of Wave Transmission and Reflection Characteristics of Laboratory Breakwaters.” TR 80-1, USACE, CERC, Fort Belvoir, Va.

Smith, Katharine A., et al. “Modeling the Effects of Oyster Reefs and Breakwaters on Seagrass Growth.” *SpringerLink*, Springer-Verlag, 23 May 2009, link.springer.com/article/10.1007/s12237-009-9170-z.

Sternberg, R.W., 1968. Friction factors in tidal channels with different bed roughness. Marine Geology, 6,243-263.

Turner, R. E. 1985. Relationships between coastal land losses and canals and canal levees in Louisiana and management options. Biological Services Program, US Fish and Wildlife Service, Washington, DC. FWS/OBS-85. 71 pp.

USGS Fact Sheet 1995 “Louisiana Coastal Wetlands: A Resource At Risk.” *USGS Publications Warehouse*, U.S. Geological Survey Pacific Northwest Urban Corridor Mapping Project, pubs.usgs.gov/fs/la-wetlands/.

Van der Meer, J. W., Briganti, R., Zanuttigh, B., & Wang, B. (2005). Wave Transmission and Reflection at Low-Crested Structures: Design Formulae, Oblique Wave Attack, and Spectral Change. Coastal Engineering , 52, 915- 929.

Van der Meer, J., & d'Angremond, K. (1992). Wave Transmission at Low Crested Stuctures. Costal Structures and Breakwaters (pp. 25-41). London: Institution of Civil Engineers.

Van Dongeren, A.R., Lowe, R.J., Pomeroy, A., Trang D.M., Roelvink, J.A., Symonds, G., and Ranasinghe, R., 2012. , *Coastal Engineering Proceedings*, [S.I.], n. 33, p currents. ISSN 2156-1028.

Webb, B.M. and Allen, R. (2015). Wave transmission through artificial reef breakwaters. *Coastal Structures and Solutions to Coastal Disasters 2015: Resilient Coastal Communities* 432-441.

Xiankun, Ke, et al. "Velocity Structure and Sea Bed Roughness Associated with Intertidal (Sand and Mud) Flats and Saltmarshes of the Wash, U.K. ." *Journal of Coastal Research*, vol. 10, no. 3, 2 Dec. 1993, pp. 702–715., doi:http://journals.fcla.edu/jcr/article/download/79440/76774.

APPENDIX A. VOLUMETRIC CHANGE RATE EXAMPLE FIGURES

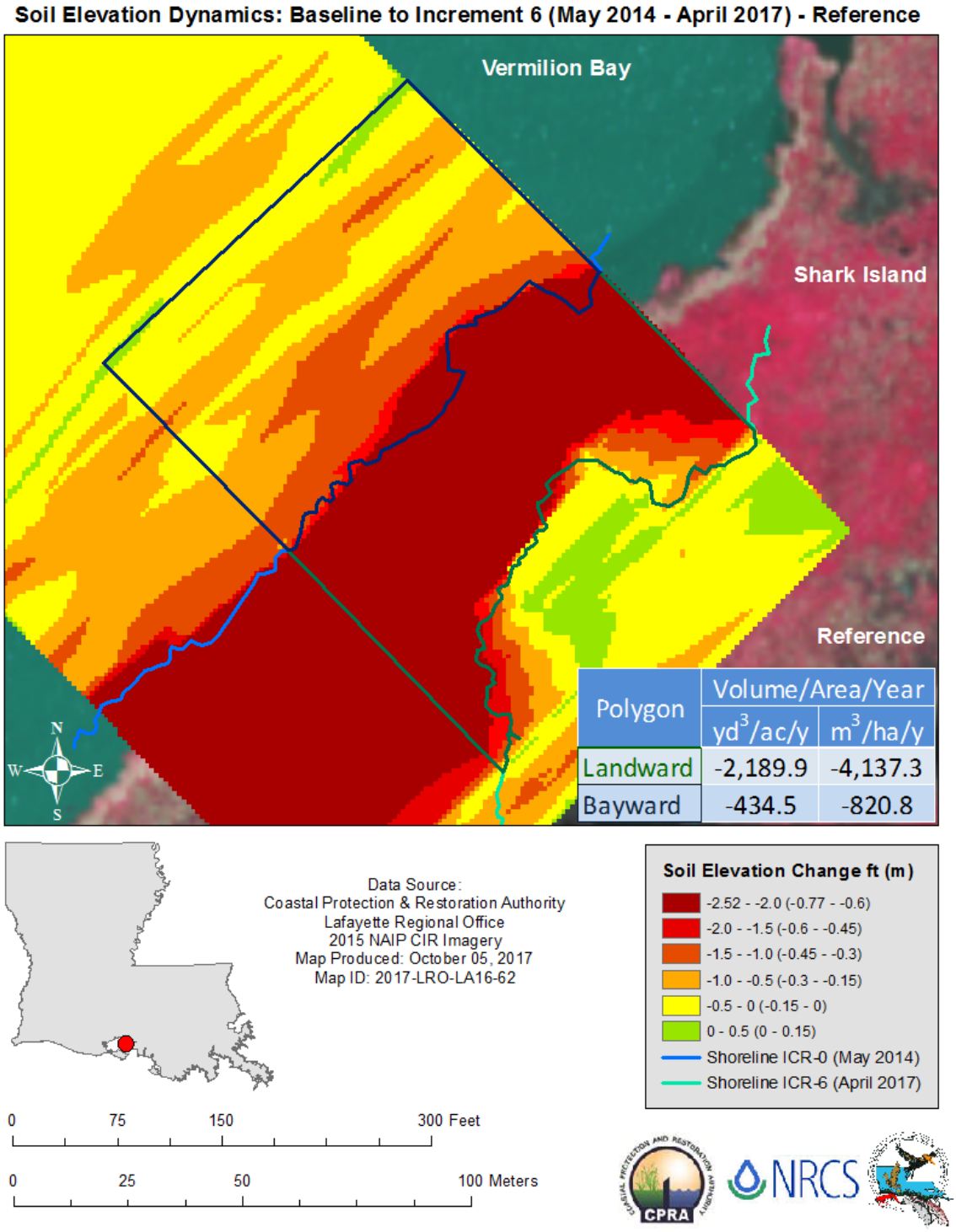

Figure 5. Soil elevation change was mapped in the Reference area of the Non-rock Alternatives to Shoreline Protection Demonstration Project (LA-0016) for the 3-year monitoring period (May 2014 - April 2017). The table displays volume change rates of the inset polygons.

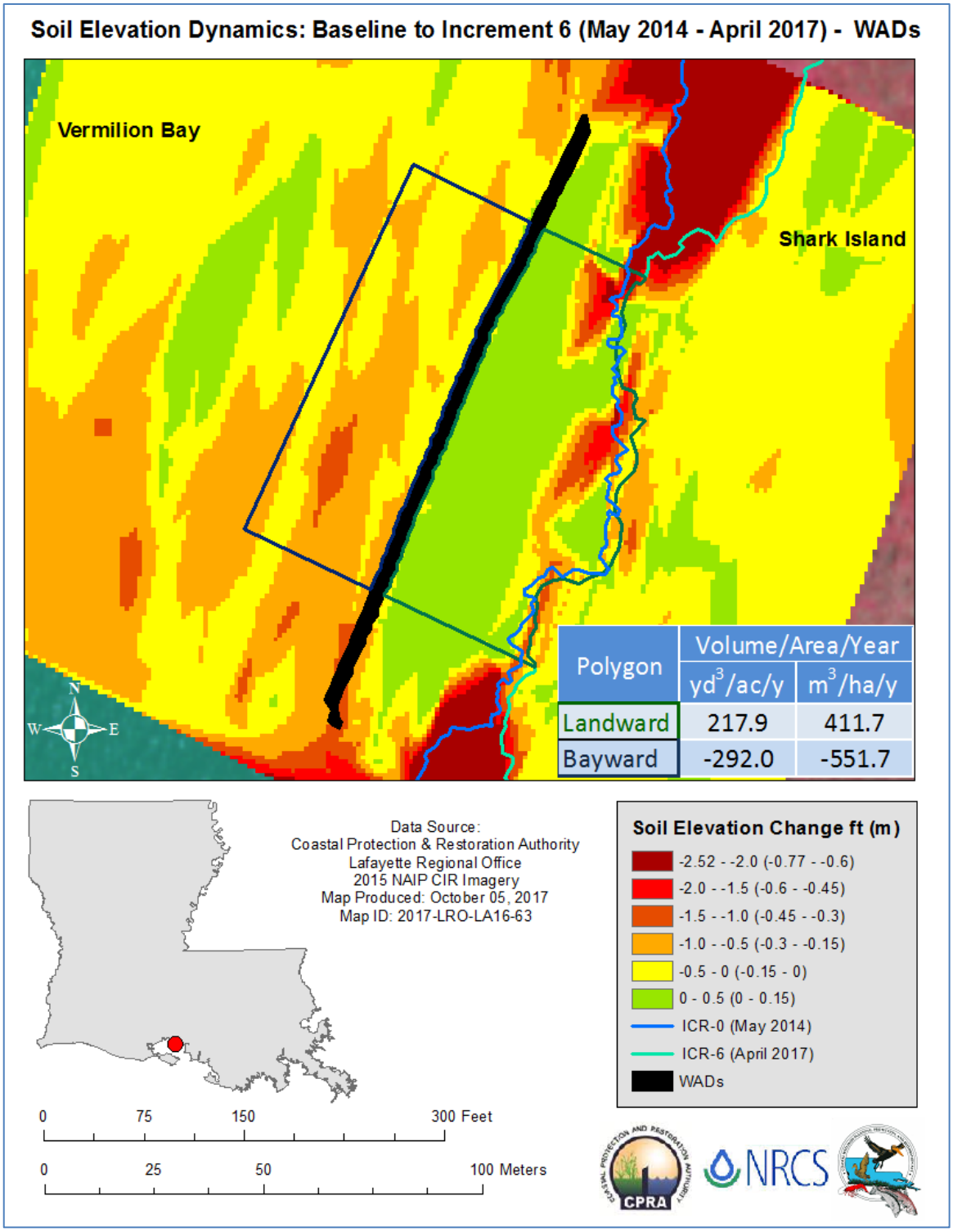

Figure 10. Soil elevation change was mapped in Living Shoreline Solutions' Wave Attenuation Devices (WAD®s) area of the Non-rock Alternatives to Shoreline Protection Demonstration Project (LA-0016) for the 3-year monitoring period (May 2014 - April 2017). The table displays volume change rates of the inset polygons.

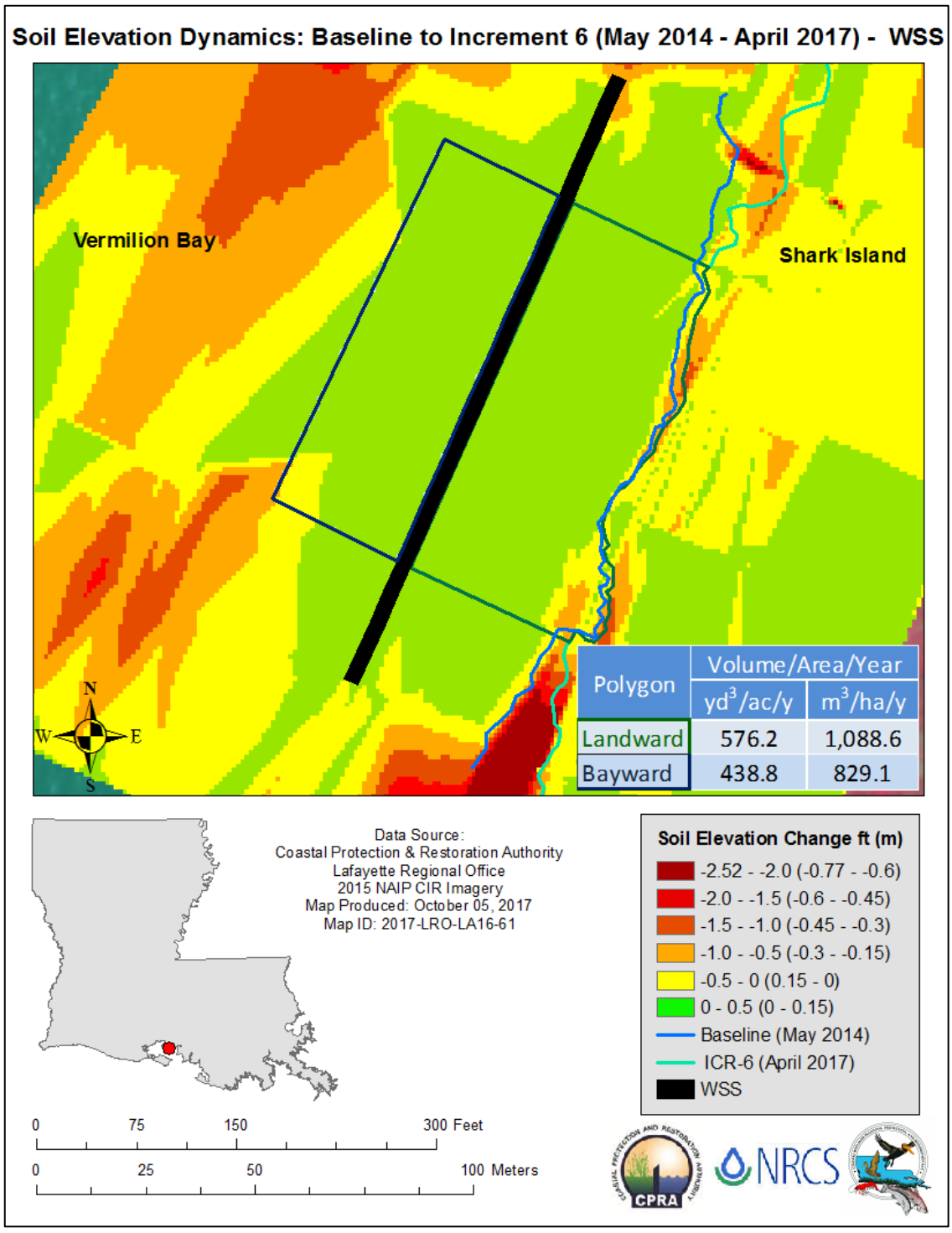

Figure 15. Soil elevation change was mapped in Integrated Shoreline Solutions' Wave Screen System (WSS) area of the Non-rock Alternatives to Shoreline Protection Demonstration Project (LA-0016) for the 3-year monitoring period (May 2014 - April 2017). The table displays volume change rates of the inset polygons.

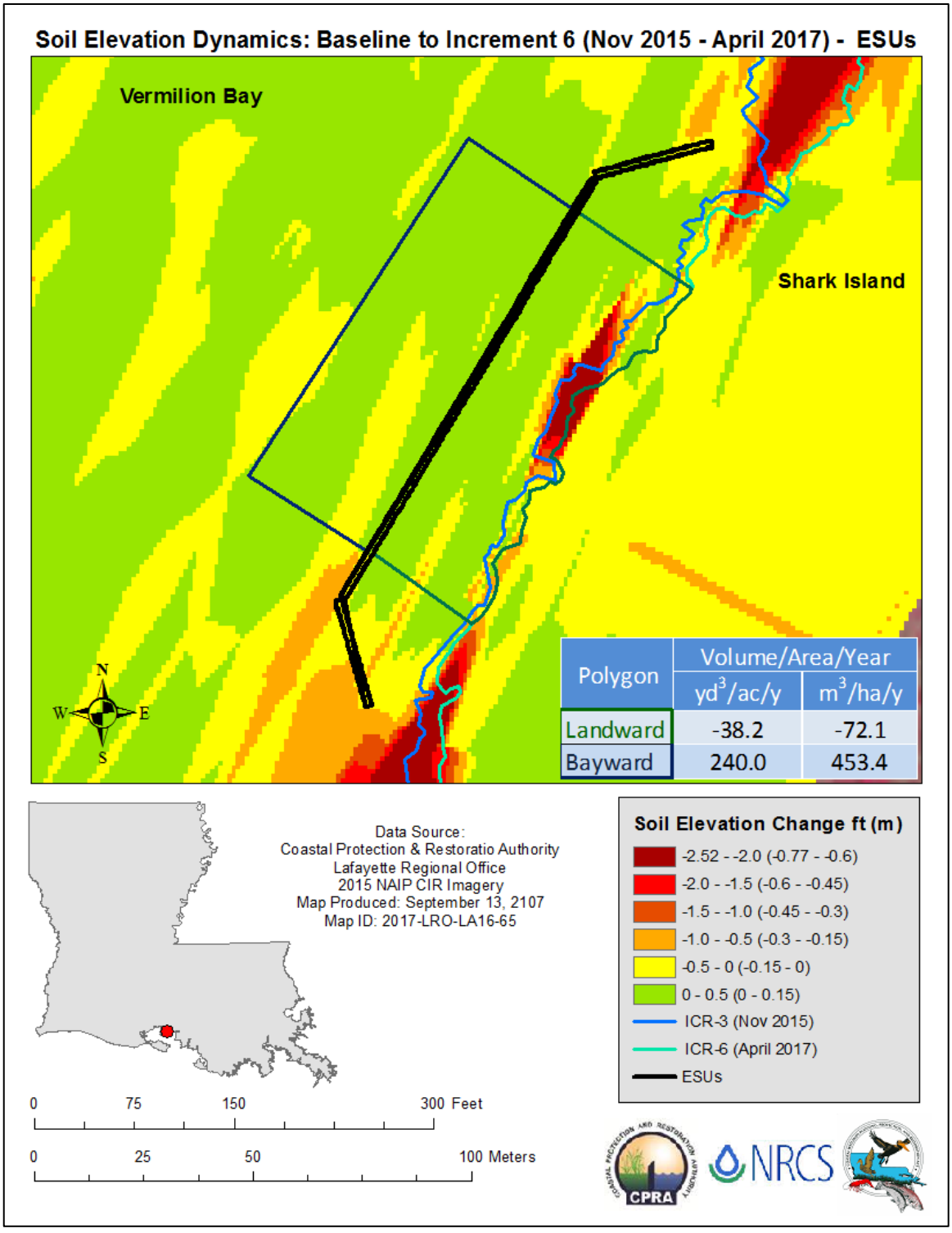

Figure 20. Soil elevation change was mapped in Walter Marine's EcoSystem Units (ESUs) area of the Non-rock Alternatives to Shoreline Protection Demonstration Project (LA-0016) for the one and one-half year monitoring period (Nov 2015 - April 2017). The table displays volume change rates of the inset polygons.

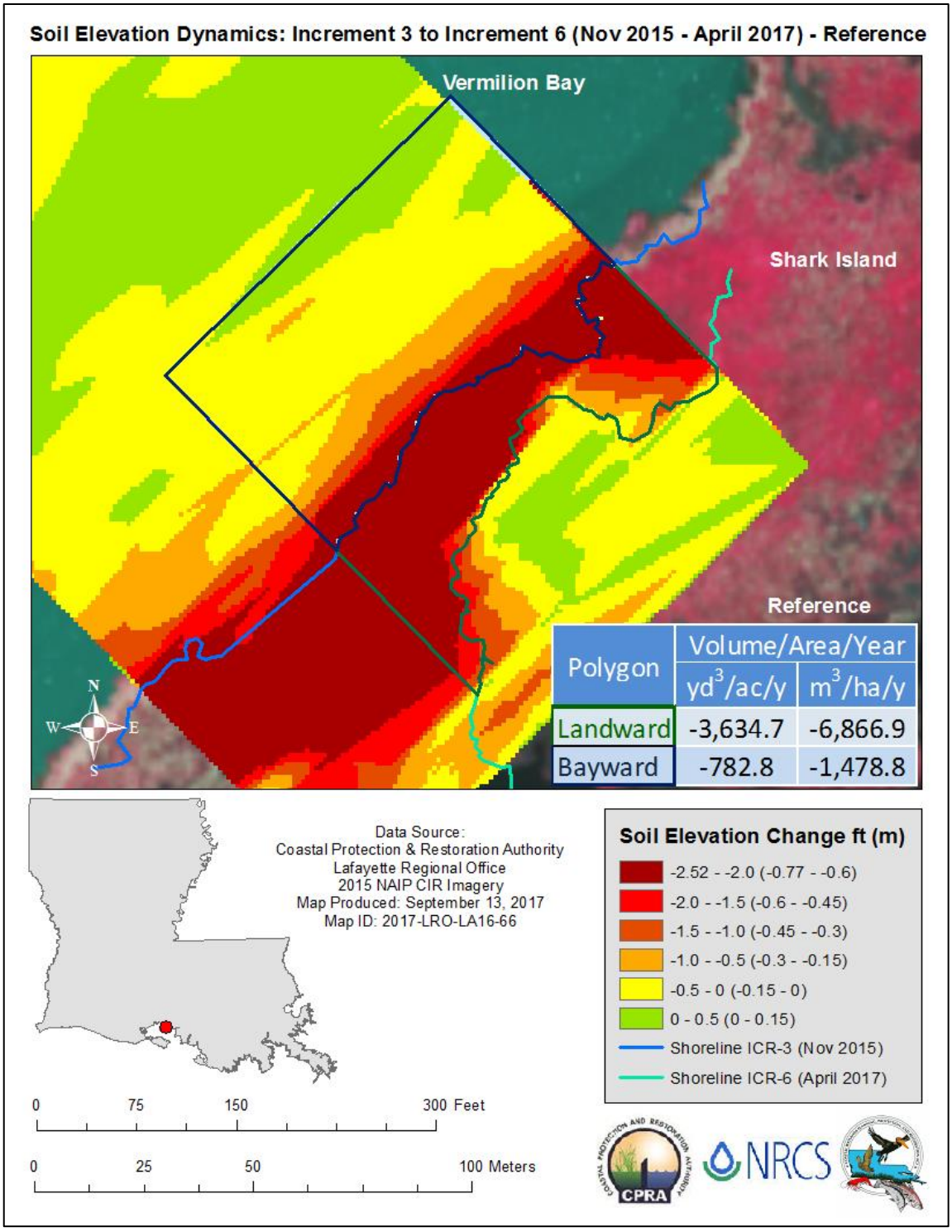

Figure 21. Soil elevation change was mapped in the Reference area of the Non-rock Alternatives to Shoreline Protection Demonstration Project (LA-0016) for a one and one-half year monitoring period (Nov 2015 - April 2017). The table displays volume change rates of the inset polygons on either side of the November 2015 shoreline.

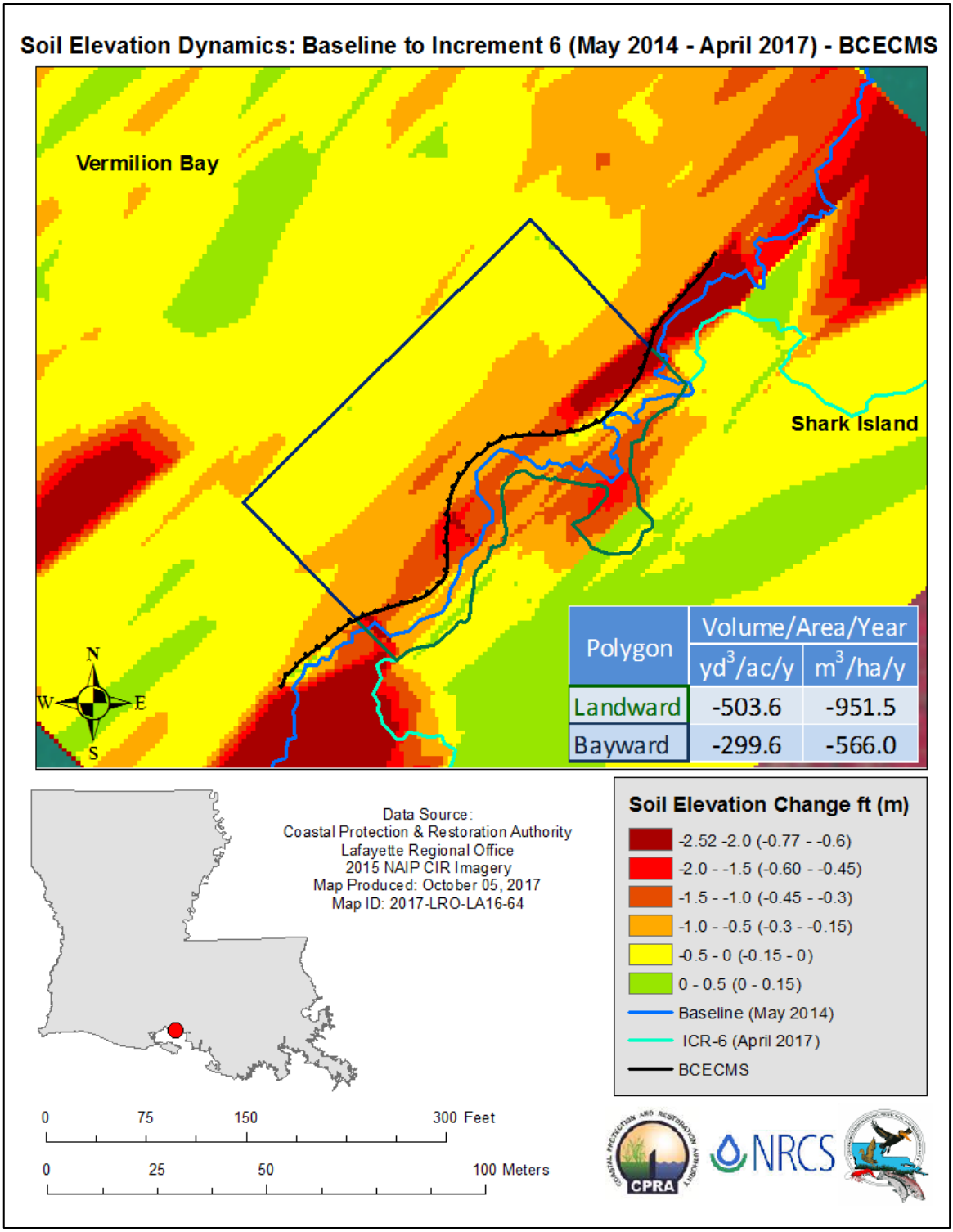

Figure 26. Soil elevation change was mapped in Jansen, Inc.'s Buoyancy Compensated Erosion Control Modular System (BCECMS) area of the Non-rock Alternatives to Shoreline Protection Demonstration Project (LA-0016) for the 3-year monitoring period (May 2014 - April 2017). The table displays volume change rates of the inset polygons.

APPENDIX B. EXAMPLE CALCULATIONS

PO-0148 Porosity Coefficient Example Calculations

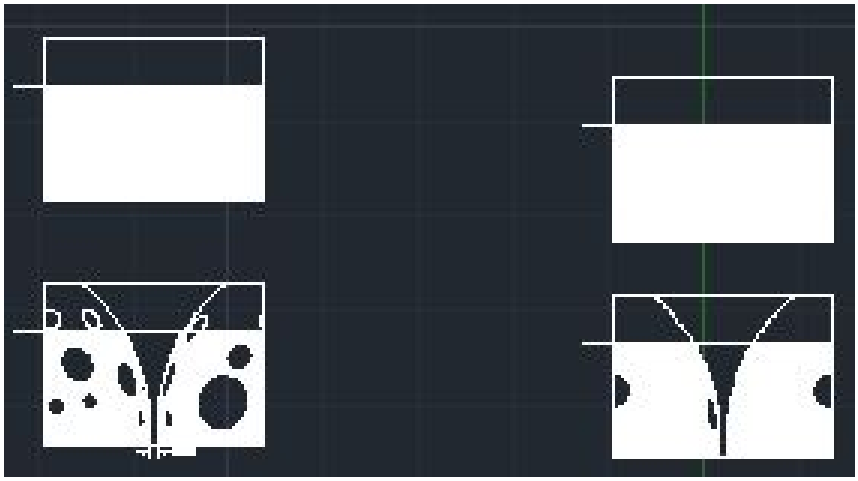

Reef Ball Type 1

From Autocad Drawing:

Blocked Area = 11.414 square feet

Total Area =17.25 square feet

Unblocked Area = 5.836 square feet

Porosity Coefficient = 5.836/17.25 = 33.83%

Reef Ball Type 2

From Autocad Drawing:

Blocked Area = 14.5291 square feet

Total Area =17.25 square feet

Unblocked Area= 2.72 square feet

Porosity Coefficient = 2.72/17.25 =15.77%

Example Soil Volume Change Rate Calculation

Average bathymetry survey change = 22.99 square feet

Average change over middle 300 foot section = 22.99 square feet * 300 ft

=6897.00 cubic feet

Average volume change converted to yards = 255.44 cubic yards

Time between bathymetry surveys = 1 year 2 months = 1.17 years

Average Volume Change Rate per year = 255.44 / 1.17 years

= 218.32 cubic yards / year

Distance from Structure to Shore = 119.3 feet

Area of middle 300 foot section to shoreline = 300 feet * 119.3 feet = 35790 square feet

Converted to Acres = 35790 square feet/ 435960 (Square feet / acre) = 0.8216 acres

Average soil volume change rate = 218.32 (cubic yards / year) / .8216 (acres)

= 265.77 cubic yards / acre / year

VITA

Hunter Shows is from Baton Rouge, Louisiana, and grew up hunting and fishing in the south Louisiana marshes with his family. He has seen first hand the fast rate of land loss in his time spent outdoors in Louisiana's estuaries, and has always had a passion for helping to better the environment. Hunter graduated from Catholic High School of Baton Rouge in May of 2012 and graduated from Louisiana State University in December of 2016 with a Bachelor of Science degree in Petroleum Engineering. He anticipates graduating from Louisiana State University with a Master of Science degree in Coastal and Ecological Engineering in August of 2019.

Hunter currently works for Delta Land Services, LLC as a Wetland Restoration E.I., and has worked there for the entirety of his time spent as a graduate student at Louisiana State University. He has experience in topographic surveying of various wetland, stream, and marsh sites, as well as project management, GIS and AutoCAD mapping, hydrologic and hydrogeomorphic modeling and model assessment.